

NASA
TP
1820

NASA Technical Paper 1820

LOAN COPY R
AFWL TECHN
AIRPLANE AIL

0134960



TECH LIBRARY KAFB, NM

Charts for Determining Potential Minimum Sonic-Boom Overpressures for Supersonic Cruise Aircraft

Christine M. Darden

MARCH 1981

NASA



NASA Technical Paper 1820

Charts for Determining Potential Minimum Sonic-Boom Overpressures for Supersonic Cruise Aircraft

Christine M. Darden
Langley Research Center
Hampton, Virginia



National Aeronautics
and Space Administration

**Scientific and Technical
Information Branch**

1981

SUMMARY

Charts are presented which will provide a rapid estimation of minimum achievable sonic-boom levels for supersonic cruise aircraft. These charts were obtained by using a minimization method based on modified linear theory. Results are shown for several combinations of Mach number, altitude, and aircraft length and weight. For each of these conditions, overpressure and impulse values are given for two types of sonic-boom signatures: (1) a "flat-top" or minimum-overpressure signature which has a pressure plateau behind the initial shock and (2) a minimum-shock signature which allows a pressure rise after the initial shock. Some results are also given for the effects of nose shape. An example of the use of the charts has been included.

INTRODUCTION

Sonic-boom minimization research has led to the following significant developments. The concepts of "signature freezing" (ref. 1) and a far-field minimum boom (ref. 2) combined with the basic sonic-boom theory (refs. 3 and 4) led to the mid-field minimization theory of reference 5. These results, initially limited to an isothermal atmosphere, were first modified to provide for signature propagation in the standard atmosphere (ref. 6) and then modified again to permit trade-offs between sonic-boom shock levels and nose bluntness by introducing the concept of "nose-length" ratios (ref. 7). The computer program incorporating the above theories, as presented in reference 7, calculates both the minimizing-pressure signature and the required equivalent-area distribution for a given cruise Mach number, altitude, and aircraft length and weight. Using area distributions from this program as constraints for the design of three low-boom wind-tunnel models, this minimization procedure has been verified experimentally (refs. 8 and 9).

To allow rapid evaluation of the minimum sonic-boom characteristics available at cruise for transport aircraft, this report provides a convenient series of charts which show overpressure levels, shock levels, and impulse levels for minimum-overpressure signatures and two different minimum-shock signatures. Also included are results for three different "nose-length" ratios. The charts cover a range of Mach numbers, altitudes, and aircraft lengths and weights which are believed to be typical values for future generation supersonic transports.

SYMBOLS

Values are given in both SI and U.S. Customary Units. The measurements and calculations were made in U.S. Customary Units.

A_e equivalent area
 C_D drag coefficient

h	airplane altitude
I	impulse of pressure signature, $\int_{\Delta p > 0} \Delta p \, dt$
k	reflection factor
l	equivalent length
M	Mach number
Δp	overpressure
W	airplane weight
x	axial distance
λ	nose-bluntness parameter
η	relative rise in pressure behind the initial shock in pressure signature ($0 < \eta < 1$, see ref. 7)

Subscripts:

l	equivalent length at l
o	minimum overpressure signature
r	reference conditions
s	minimum shock signature
max	maximum overpressure in minimum shock signature

MINIMUM SONIC BOOM

Types of Signatures

The term "minimum sonic boom" is ambiguous in that at least three different values of the pressure signature may be minimized: (1) the initial shock, (2) the overpressure level, and (3) the impulse. The differences in the resulting signature shapes are quite significant, depending on which value is minimized. Results for the first two of these signature shapes are presented in this paper. If the overpressure is minimized, the associated pressure signature is flat from the initial shock to the expansion region of the signature as illustrated in figure 1. If the shock is minimized, then overpressure levels are allowed to rise following the initial shock. The rate of rise in this signature is controlled by η which can have a value from 0 to 1.0 (ref. 7). When η has a value of 1.0, the resulting signature is an "N-wave." An η value of zero indicates a "flat-top" signature. Typical variations of impulse and initial shock with η are shown in figure 1. Note that the initial shock Δp decreases linearly with η and that impulse I increases linearly with η .

Recent experimental work at the University of Toronto on "outdoor-disturbance" levels indicates that pressure rises following the initial shock add very little additional disturbance (ref. 10). These pressure rises do, however, produce large benefits in airplane weight. In these experiments, minimum-shock signatures developed by the methods of reference 7 were produced on a loud-speaker driven system and human reaction to the boom levels were obtained.

Vehicle Parameters

The minimizing-area distribution and, thus, the resulting pressure signatures are affected greatly by the airplane length, weight, and "nose-length." Results shown in figure 2 clearly indicate that lower weights and/or increased lengths will significantly improve the sonic-boom characteristics of an aircraft. These results were obtained using the "flat-top" signature, but trends are the same when the minimum-shock signature is calculated.

As discussed in reference 5, the equivalent area for minimum sonic boom has an infinite gradient at $x = 0$. This bluntness is not consistent with shapes needed for low wave drag. As a compromise, a nose-bluntness parameter λ or "nose-length" ratio is defined (ref. 8). A value of $\lambda = 0.1$ indicates that the area up to 1/10 the total length has been changed to a sharper cusplike region as seen in figure 3. Values of λ normally range from 0 to 0.2. The effects of these changes in the nose equivalent area on drag, overpressure, and impulse are also shown in figure 3. As the nose-bluntness parameter λ increases, levels of drag decrease as expected, but there is a corresponding increase in the levels of overpressure and impulse. This study was made with bodies of revolution corresponding to these equivalent areas being used to get approximate drag increments.

Flight Conditions

Typical effects of altitude and Mach number on overpressure and impulse levels are shown in figure 4. Note that overpressure levels increase with Mach number over the entire range shown and with altitude over most of the range shown. There is a decrease in impulse with Mach number but an increase in the equivalent area causes the impulse to increase with increasing altitude.

PRESENTATION OF CHARTS

Figures 5 to 16 of this report give results from the minimization program for flight/design parameters for typical supersonic cruise aircraft. Mach numbers range from 2.5 to 3.5, weights range from 180 000 kg to 320 000 kg (400 000 lb to 700 000 lb), altitudes range from 15 km to 30 km (50 000 ft to 100 000 ft), and lengths range from 73 m to 110 m (240 ft to 360 ft). Results are shown for minimum-overpressure signatures ($\eta = 0$) and for two minimum-shock signatures ($\eta = 0.5$ and 0.9). "Nose-length" ratios λ of 0, 0.1, and 0.2 are shown for every case. A ground reflection factor of 2 has been used in all cases. Corresponding area distributions are not presented but are available through use of the computer program of reference 7. The 1962 Standard Atmosphere

Tables (ref. 11) have been used in all calculations. The following table gives an overview of available information presented in figures 5 to 16:

Reference to charts			
Figure	Abscissa	Three values shown in charts	Constant
5	l	h	M, W
6	h	l	M, W
7	W	h	M, l
8	h	W	M, l
9	W	l	M, h
10	l	W	M, h
11	M	h	l, W
12	h	M	l, W
13	W	M	h, l
14	M	W	h, l
15	M	l	h, W
16	l	M	h, W

The base values used for perturbation of these parameters are $M = 3.2$
 $W = 283\,495$ kg (625 000 lb), $l = 94.49$ m (310 ft), $h = 24.384$ km (80 000 ft).

EXAMPLE OF CHART APPLICATION

As an example of the use of the charts, consider the determination of the best achievable sonic-boom level of an aircraft which is 94.49 m (310 ft) in length and which cruises at a Mach number of 2.7 at 18.288 km (60 000 ft). The start of cruise weight is 283 495 kg (625 000 lb). A sonic-boom estimate for these conditions using a minimum-overpressure signature is given in figure 11(a). At Mach 2.7, the best achievable Δp is about 47.3 Pa (0.99 lb/ft²). For relaxed nose bluntness, $\lambda = 0.1$ and 0.2, the values of Δp increase to 51.1 and 55.2 Pa (1.07 and 1.15 lb/ft²), respectively.

If instead of the "flat-top" signature, the intermediate finite-rise signature ($\eta = 0.5$) is chosen, the overpressure estimates are located in figure 11(b). For the blunt ($\lambda = 0$) case, the shock overpressure Δp is about 43 Pa (0.9 lb/ft²) and the corresponding maximum overpressure Δp_{\max} is about 72 Pa (1.5 lb/ft²). Again, slight increases are shown as λ increases to 0.1 and 0.2. Values of the shock Δp and the maximum overpressure for a very steep minimum-overpressure signature ($\eta = 0.9$) are seen in figure 11(c). At $\lambda = 0$, the level of Δp is about 40 Pa (0.85 lb/ft²) and the maximum overpressure level increases to roughly 93 Pa (1.94 lb/ft²). Impulse levels are read in a like manner from the corresponding figures on the right.

Quick estimates, as previously shown, can easily be made for other design/cruise parameters. The complete pressure signature and the equivalent-area distribution can be obtained by using the computer program of reference 7. The design of an aircraft to match an equivalent-area distribution is described in references 8 and 9. This equivalent area is composed of aircraft volume, lifting forces, displacement thickness, and exhaust plumes. Freedom is allowed in the arrangement of these various contributions to the total-area distribution.

The nature of the minimizing-area distribution suggests general design features which may be needed in order to meet the total area criteria. Among these design features are an extended lifting surface, blunt nose region, long equivalent length, and dihedral. Many of these features present some problems and will thus require some compromise.

Langley Research Center
National Aeronautics and Space Administration
Hampton, VA 23665
February 19, 1981

REFERENCES

1. Hayes, Wallace D.: Linearized Supersonic Flow. Ph. D. Thesis, California Inst. Technol., 1947. (Also available as North American Aviation Rep. No. AL 222.)
2. Jones, L. B.: Lower Bounds for Sonic Bangs in the Far Field. *Aeronaut. Q.*, vol. XVIII, pt. 1, Feb. 1967, pp. 1-21.
3. Whitham, G. B.: The Flow Pattern of a Supersonic Projectile. *Commun. Pure & Appl. Math.*, vol. V, no. 3, Aug. 1952, pp. 301-348.
4. Carlson, H. W.; and Maglieri, D. J.: Review of Sonic-Boom Generation Theory and Prediction Methods. *J. Acoust. Soc. America*, vol. 51, no. 2, pt. 3, Feb. 1972, pp. 675-685.
5. Seebass, R.; and George, A. R.: Sonic-Boom Minimization. *J. Acoust. Soc. America*, vol. 51, no. 2, pt. 3, Feb. 1972, pp. 686-694.
6. Darden, Christine M.: Minimization of Sonic-Boom Parameters in Real and Isothermal Atmospheres. NASA TN D-7842, 1975.
7. Darden, Christine M.: Sonic-Boom Minimization With Nose-Bluntness Relaxation. NASA TP-1348, 1979.
8. Mack, Robert J.; and Darden, Christine M.: Wind-Tunnel Investigation of the Validity of a Sonic-Boom-Minimization Concept. NASA TP-1421, 1979.
9. Mack, R. J.; and Darden, C. M.: Some Effects of Applying Sonic Boom Minimization to Supersonic Cruise Aircraft Design. *J. Aircr.*, vol. 17, no. 3, Mar. 1980, pp. 182-186.
10. Niedzwiecki, A.; and Ribner, H. S.: Subjective Loudness of "Minimized" Sonic Boom Waveforms. *J. Acoust. Soc. America*, vol. 64, no. 6, Dec. 1978, pp. 1622-1626.
11. U.S. Standard Atmosphere, 1962. NASA, U.S. Air Force, and U.S. Weather Bur., Dec. 1962.

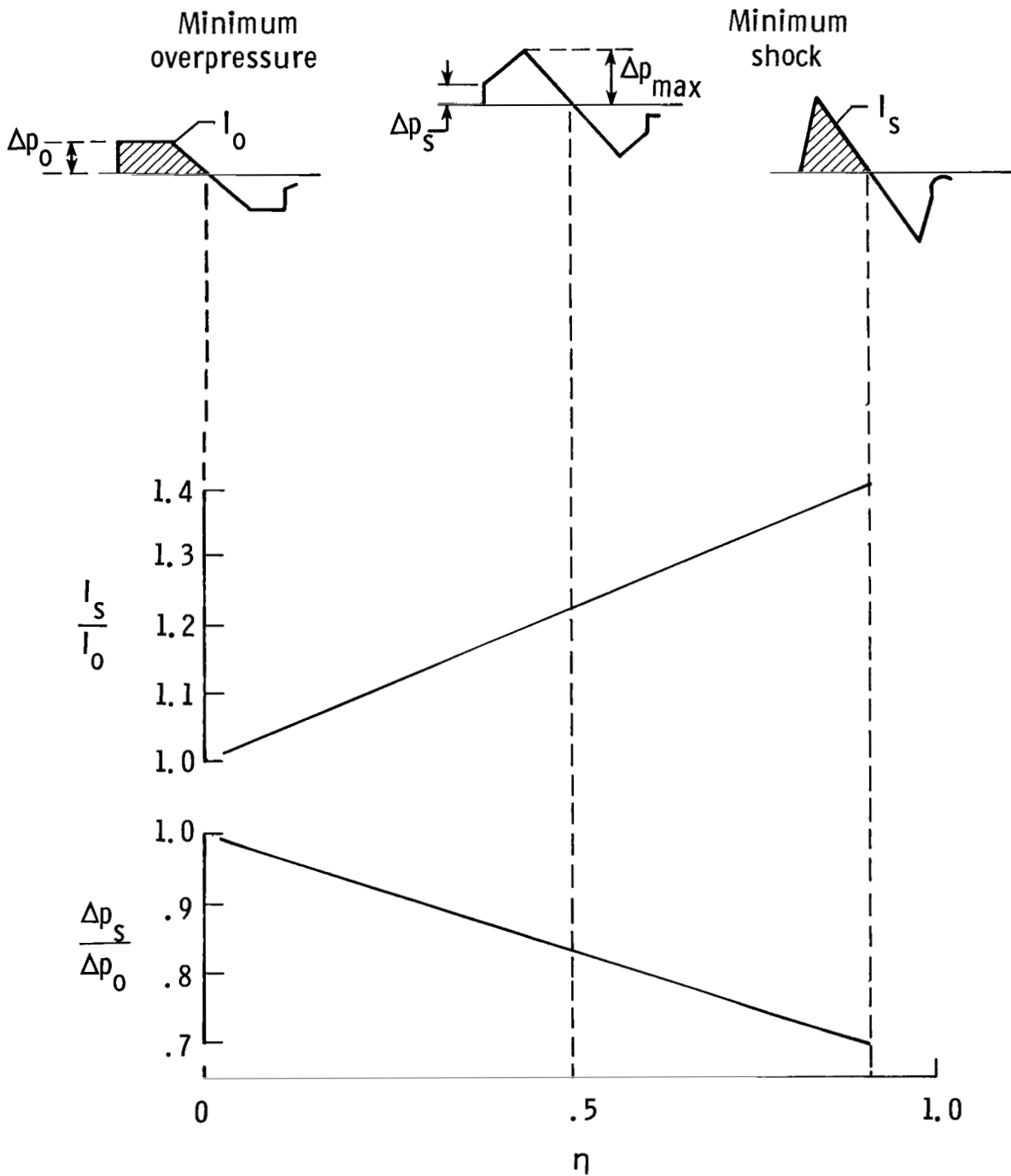


Figure 1.- Typical variations of shock and impulse levels with η .

----- Reference conditions:

$$\Delta p_r = 45.51 \text{ Pa}$$

$$I_r = 6.48 \text{ Pa-sec}$$

$$W_r = 272 \text{ 155 kg}$$

$$l_r = 91.44 \text{ m}$$

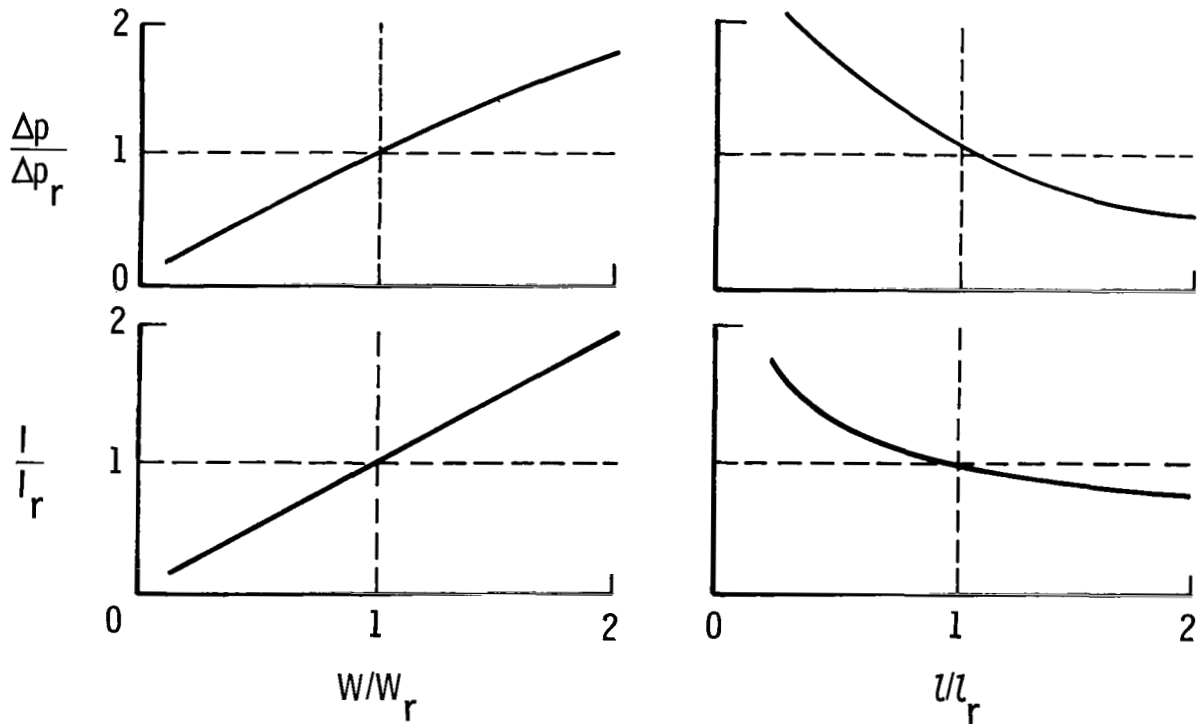


Figure 2.- Variations in sonic-boom characteristics with airplane parameters.
 $M = 2.7$; $h = 18 \text{ 288 m}$; $\eta = 0$.

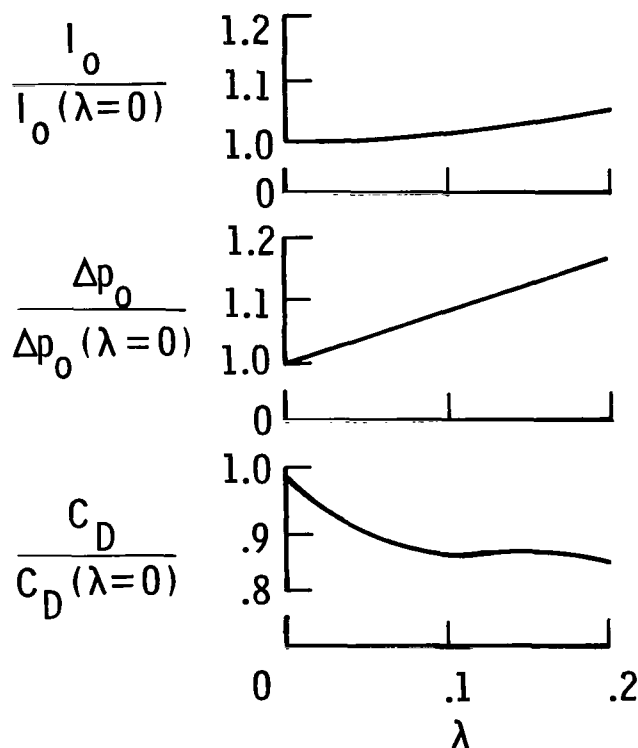
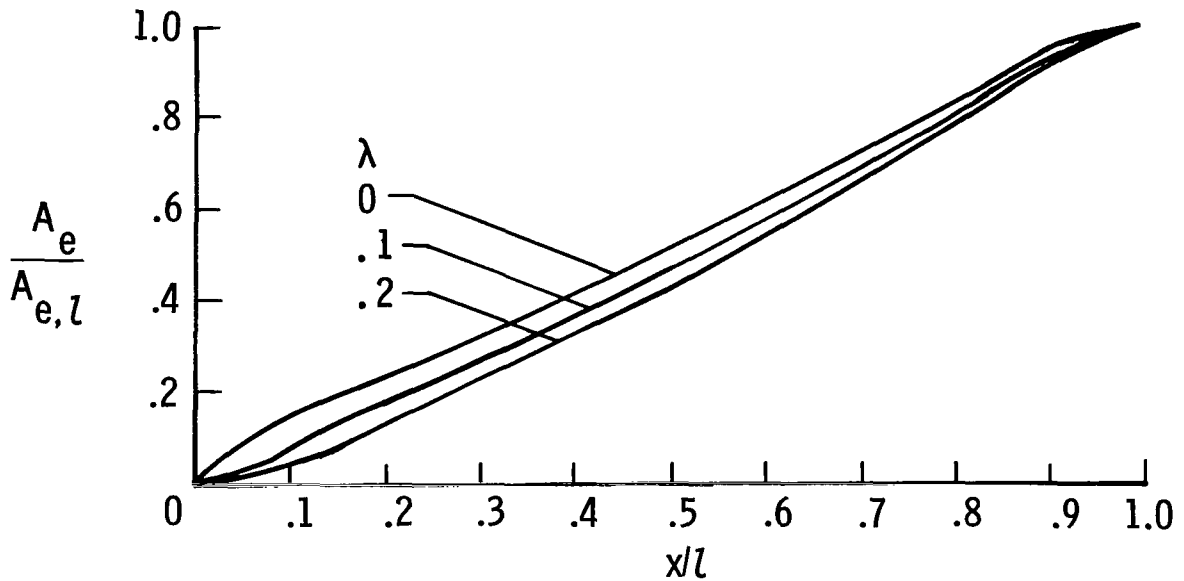


Figure 3.- Typical variations of equivalent area, sonic-boom characteristics, and drag with η . $\eta = 0$.

----- Reference conditions:

$$h_r = 18\,288 \text{ m}$$

$$M = 2.7$$

$$\Delta p_r = 45.51 \text{ Pa}$$

$$I_r = 6.48 \text{ Pa-sec}$$

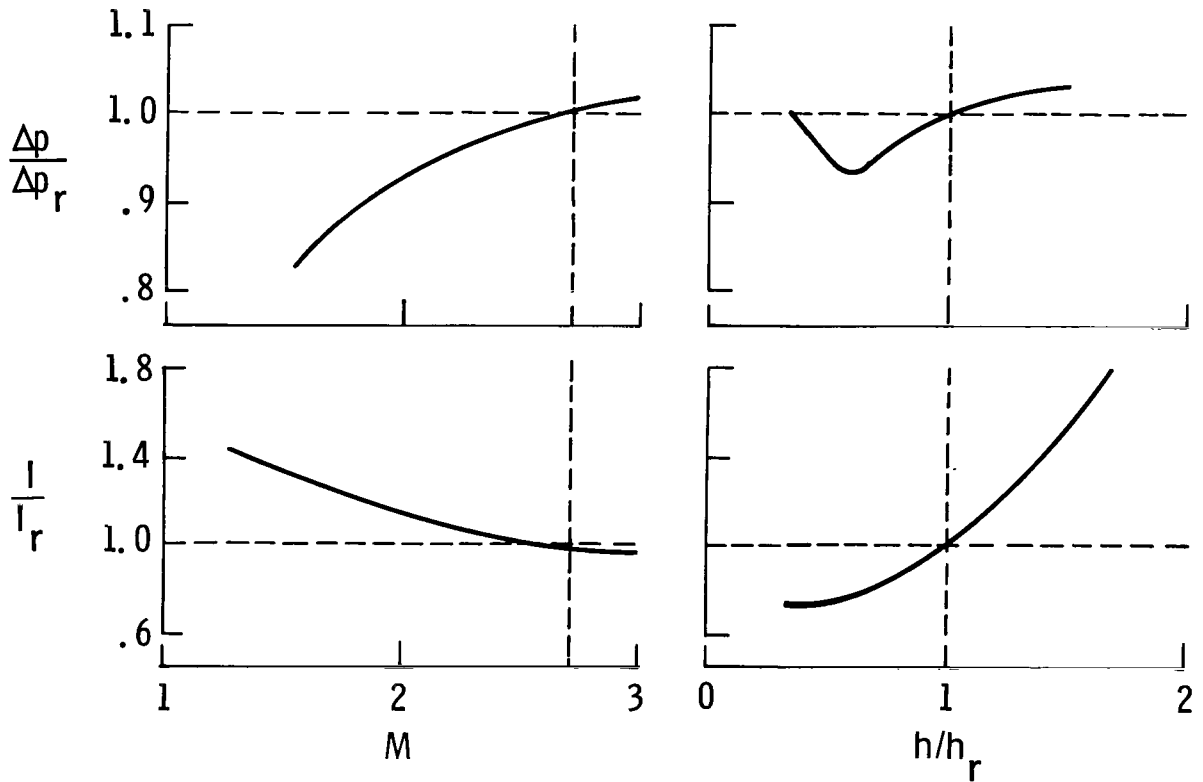
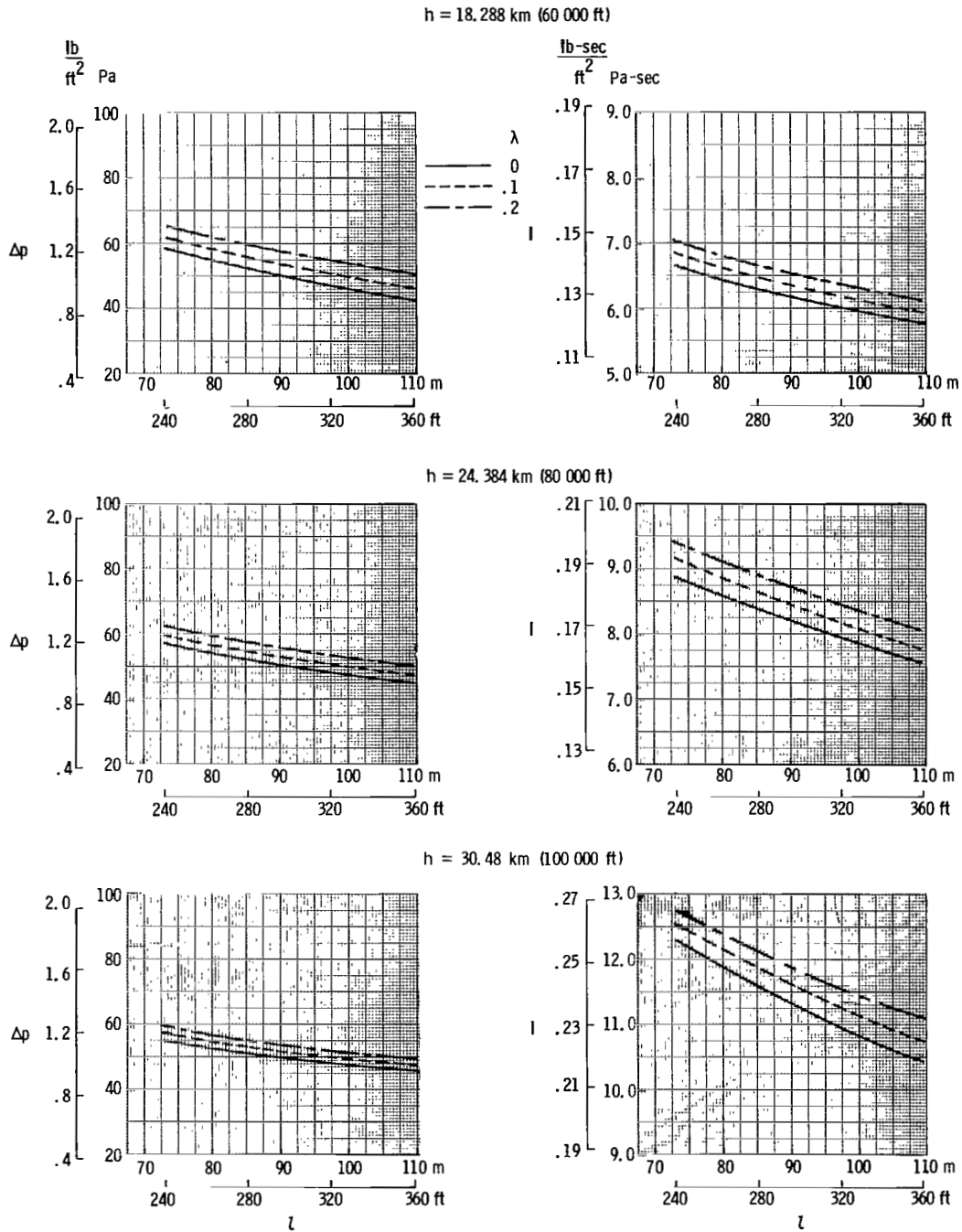


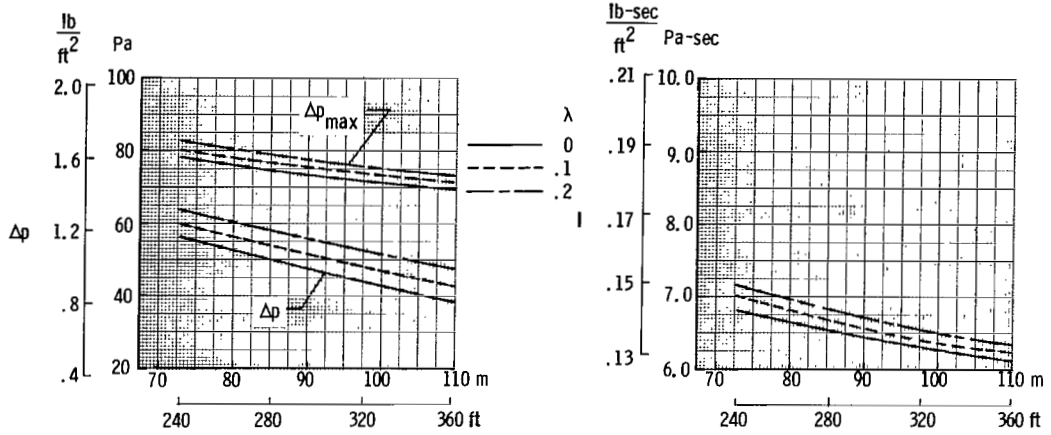
Figure 4.- Variation of sonic-boom characteristics with operational parameters.
 $W = 272\,155 \text{ kg}$; $l = 91.44 \text{ m}$; $\eta = 0$.



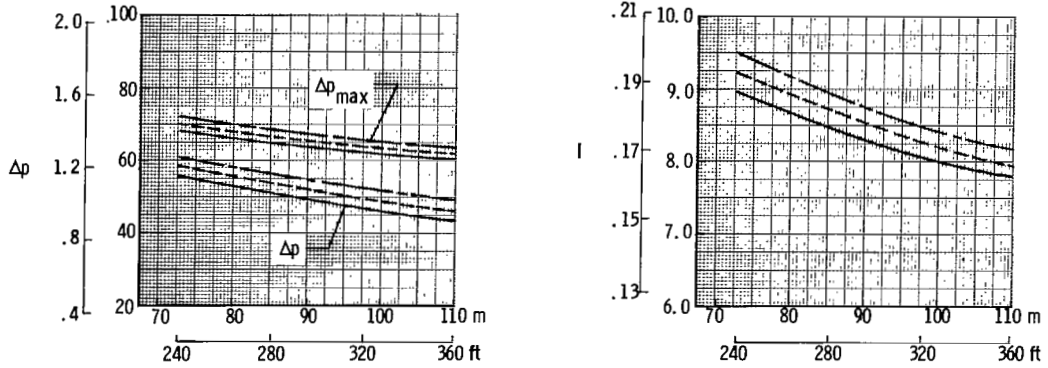
(a) "Flat-top" signature.

Figure 5.- Variation of overpressure and impulse with length. $M = 3.2$; $k = 2.0$;
 $W = 283\ 495\ \text{kg}$ (625 000 lb).

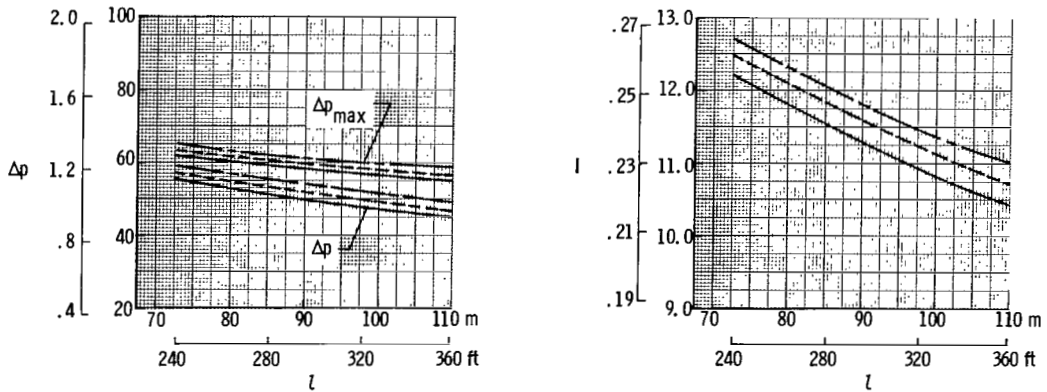
$h = 18,288 \text{ km (60 000 ft)}$



$h = 24,384 \text{ km (80 000 ft)}$



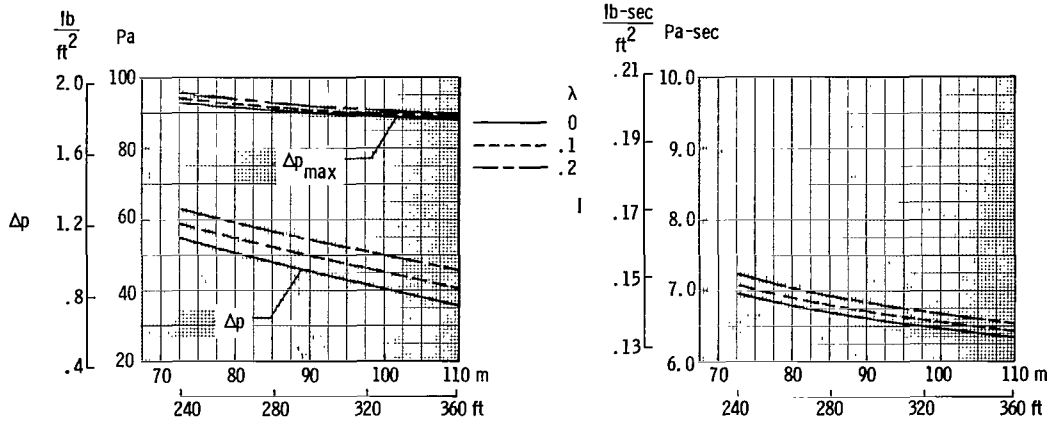
$h = 30,48 \text{ km (100 000 ft)}$



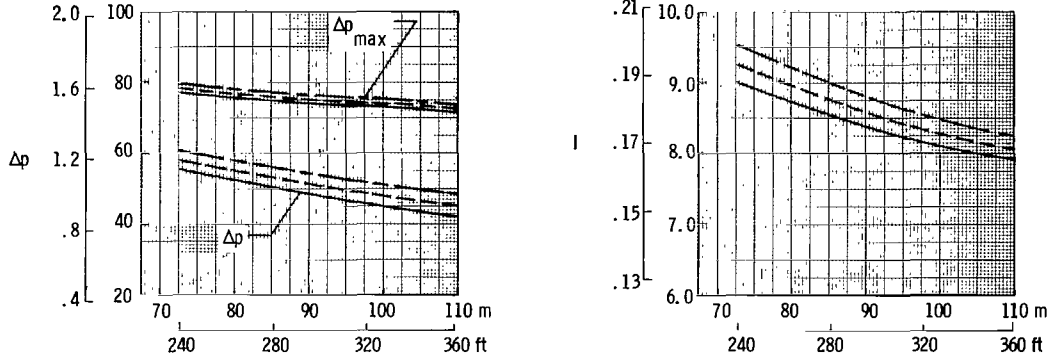
(b) Minimum-shock signature. $\eta = 0.5$.

Figure 5.- Continued.

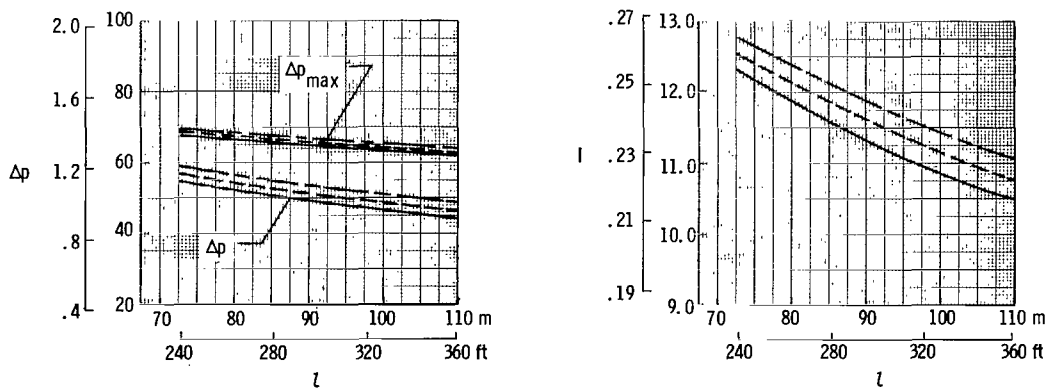
$h = 18.288 \text{ km (60 000 ft)}$



$h = 24.384 \text{ km (80 000 ft)}$

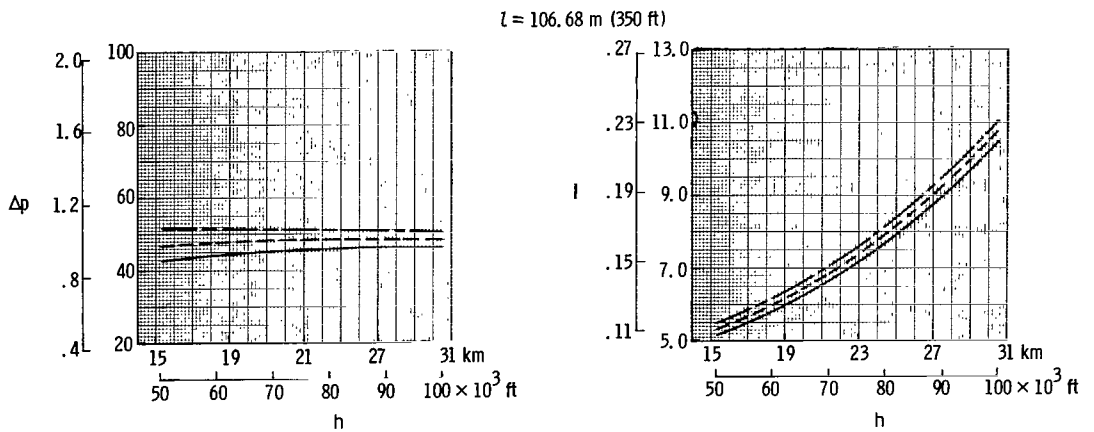
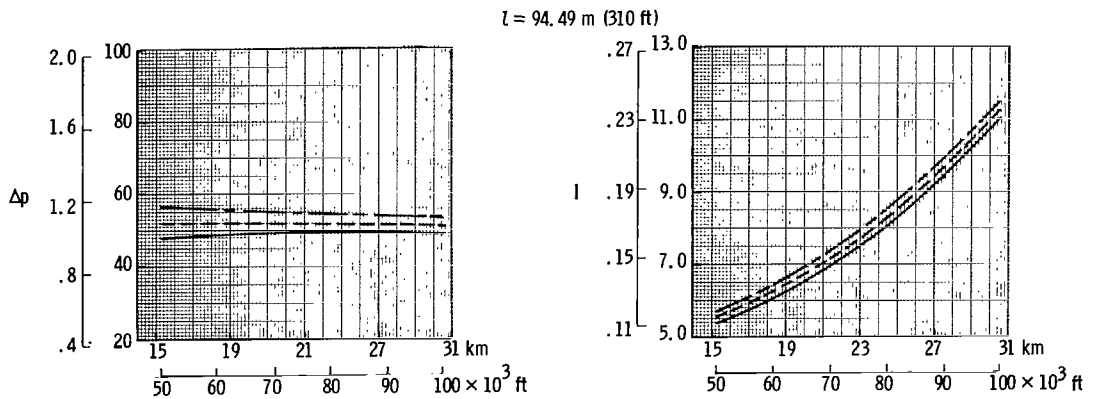
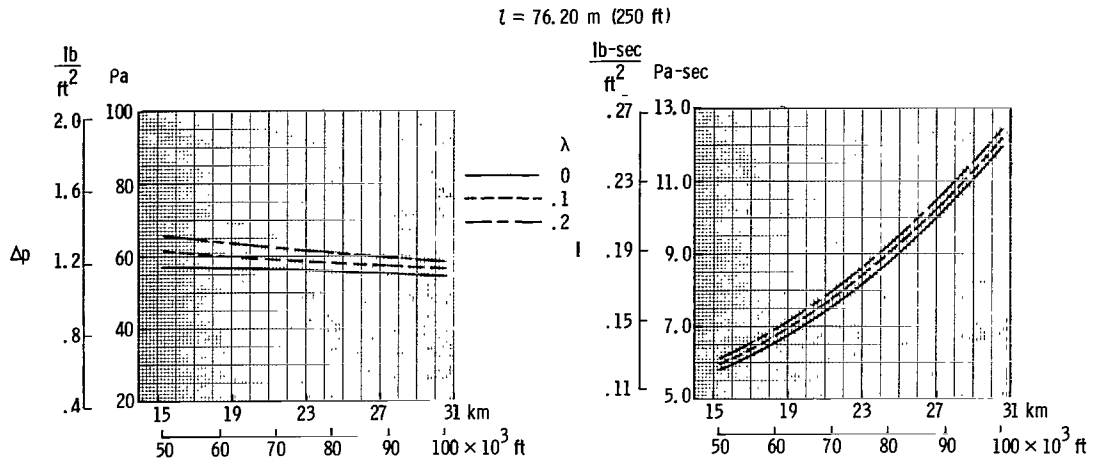


$h = 30.48 \text{ km (100 000 ft)}$



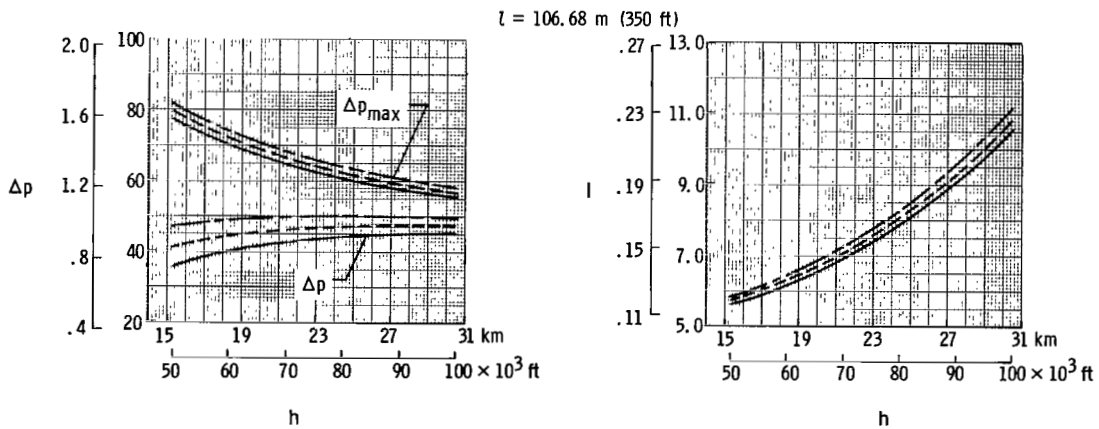
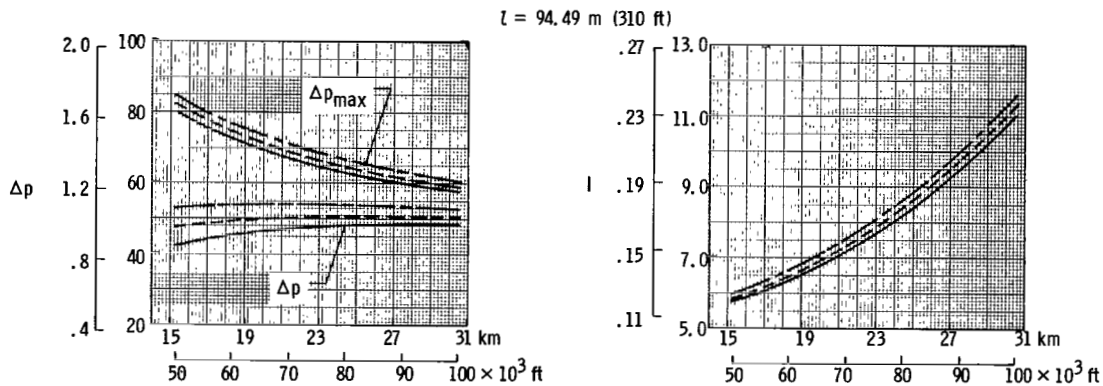
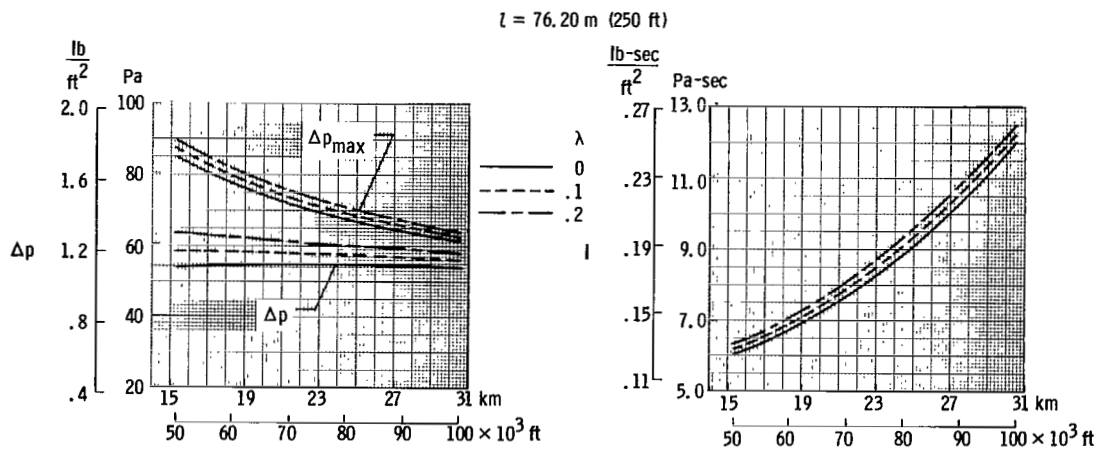
(c) Minimum-shock signature. $\eta = 0.9$.

Figure 5.- Concluded.



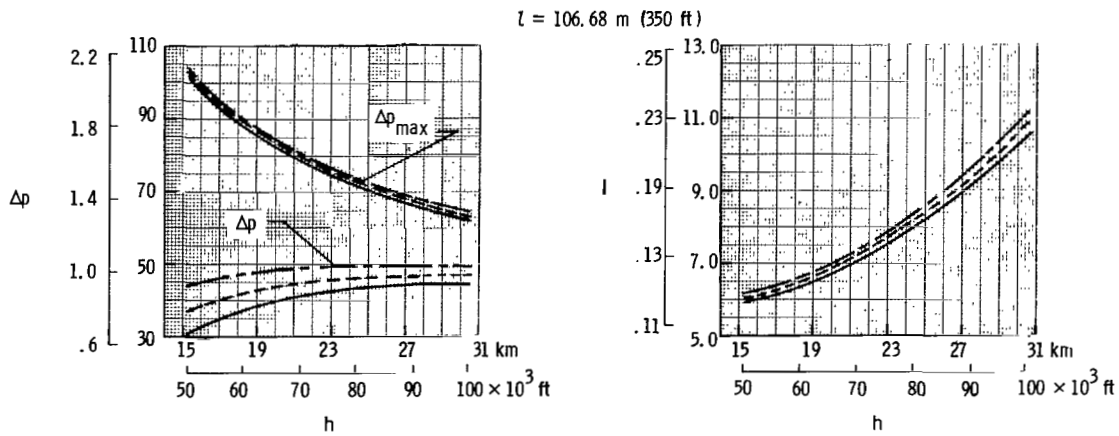
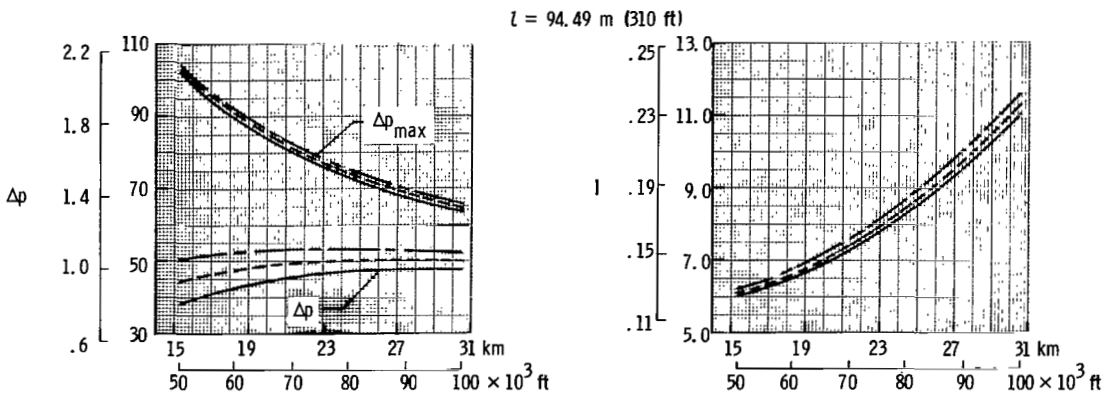
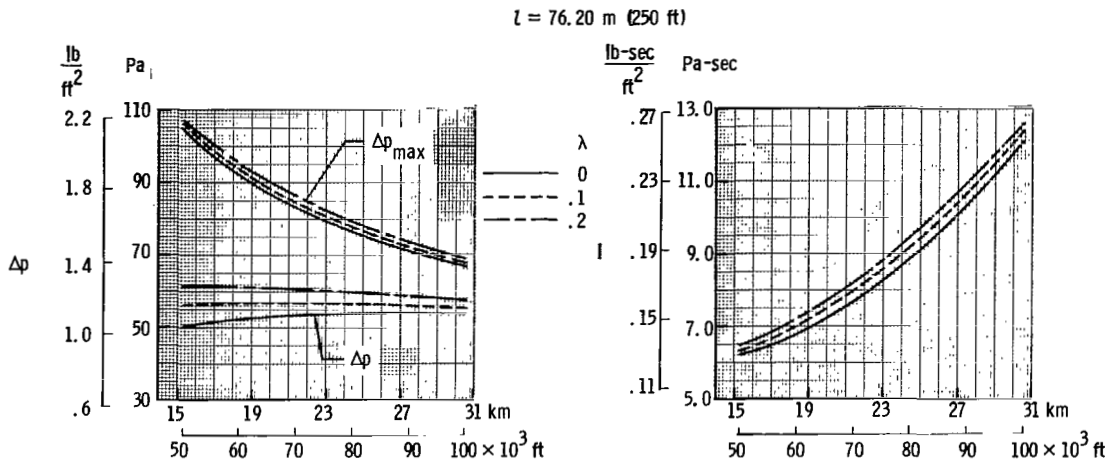
(a) "Flat-top" signature.

Figure 6.- Variation of overpressure and impulse with altitude. $M = 3.2$;
 $k = 2.0$; $W = 283\,495 \text{ kg (625\,000 lb)}$.



(b) Minimum-shock signature. $\eta = 0.5$.

Figure 6.- Continued.



(c) Minimum-shock signature. $\eta = 0.9$.

Figure 6.- Concluded.

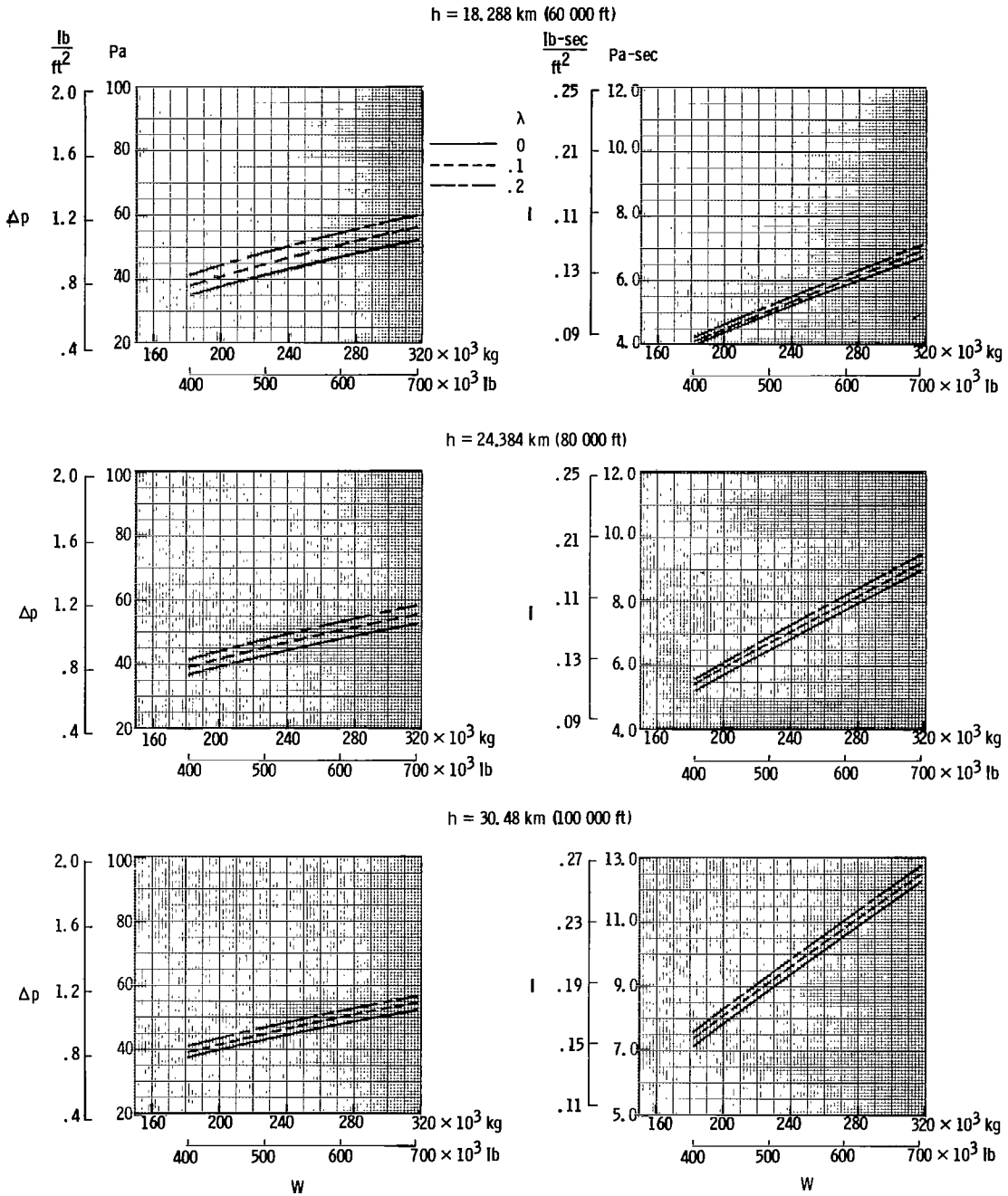
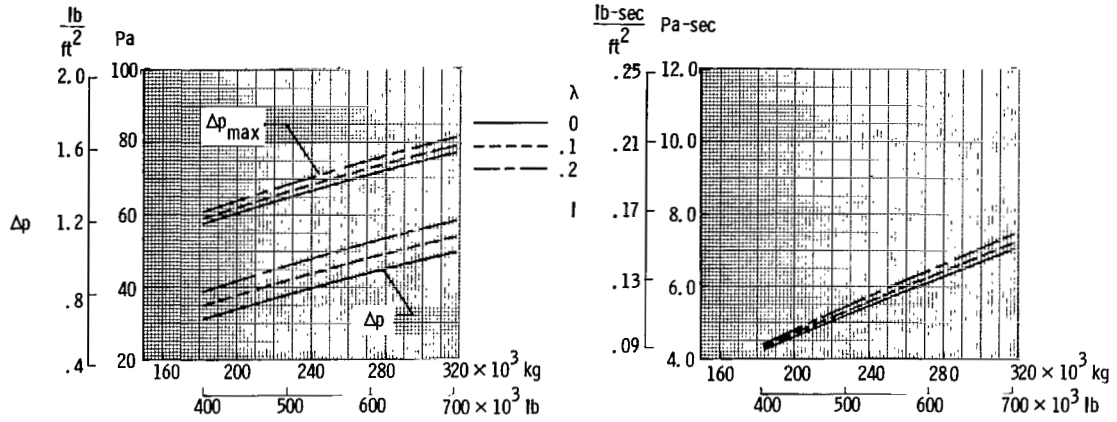
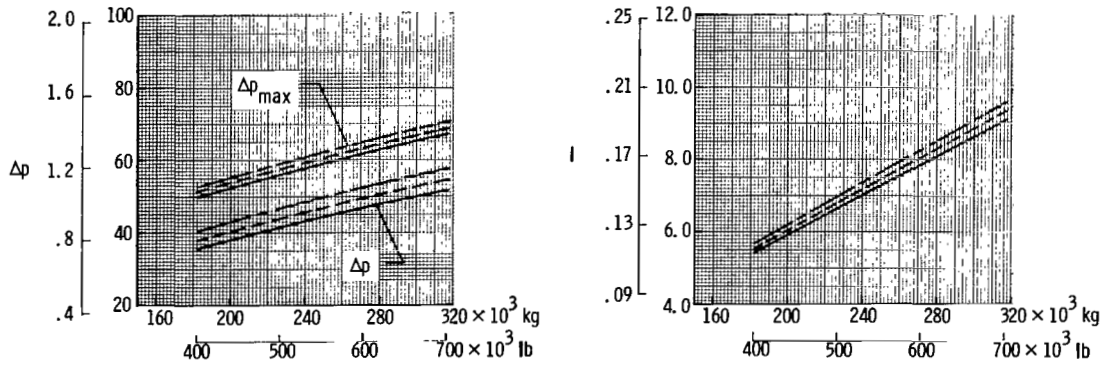


Figure 7.- Variation of overpressure and impulse with weight. $M = 3.2$; $k = 2.0$;
 $l = 94.49$ m (310 ft).

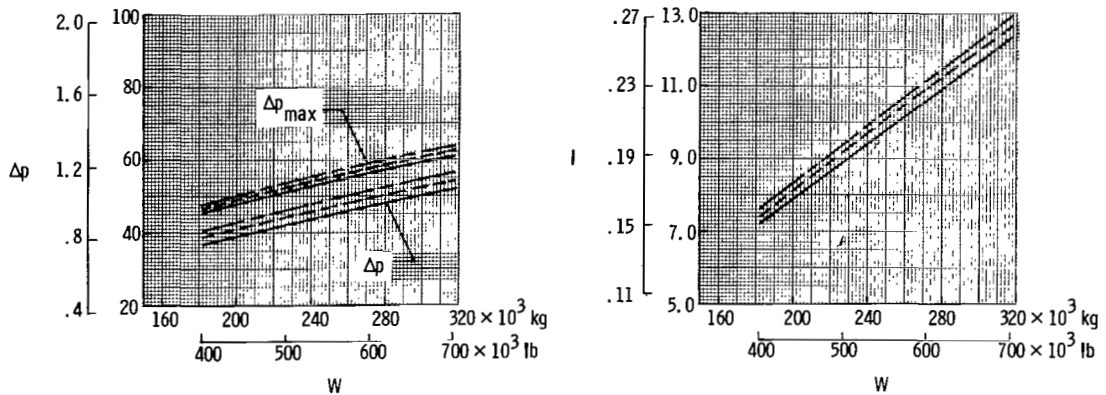
$h = 18,288 \text{ km (60 000 ft)}$



$h = 24,384 \text{ km (80 000 ft)}$



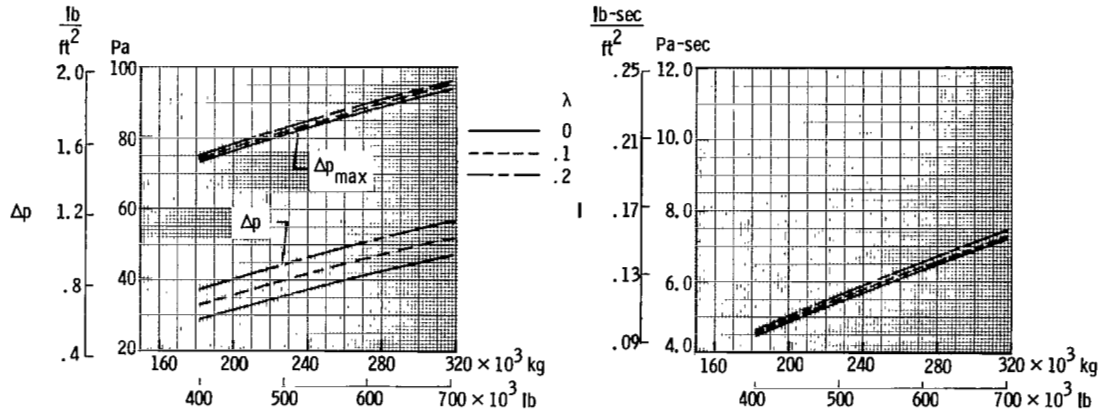
$h = 30,48 \text{ km (100 000 ft)}$



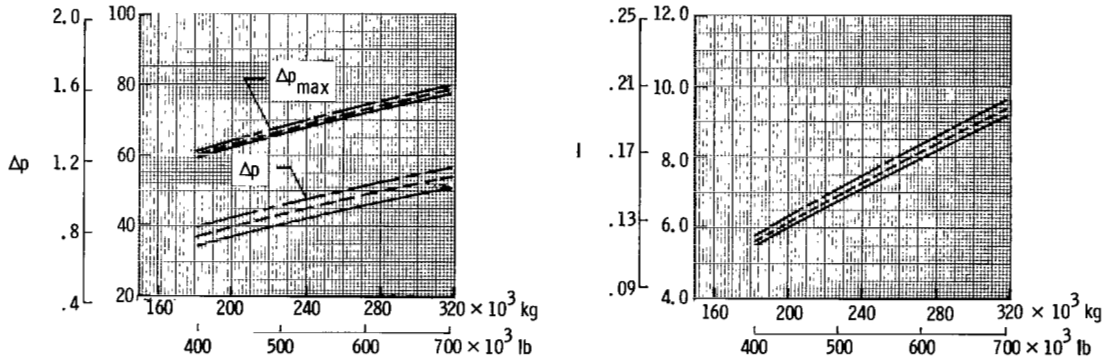
(b) Minimum-shock signature. $\eta = 0.5$.

Figure 7.- Continued.

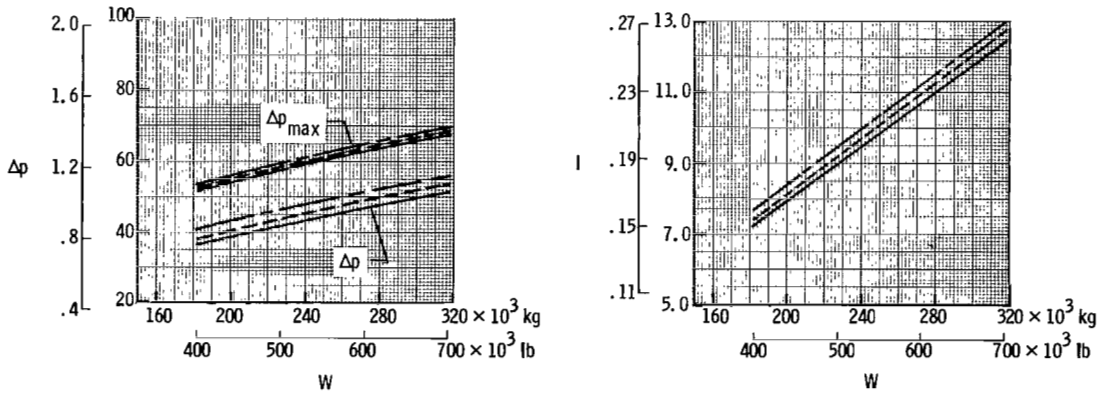
$h = 18,288 \text{ km (60 000 ft)}$



$h = 24,384 \text{ km (80 000 ft)}$

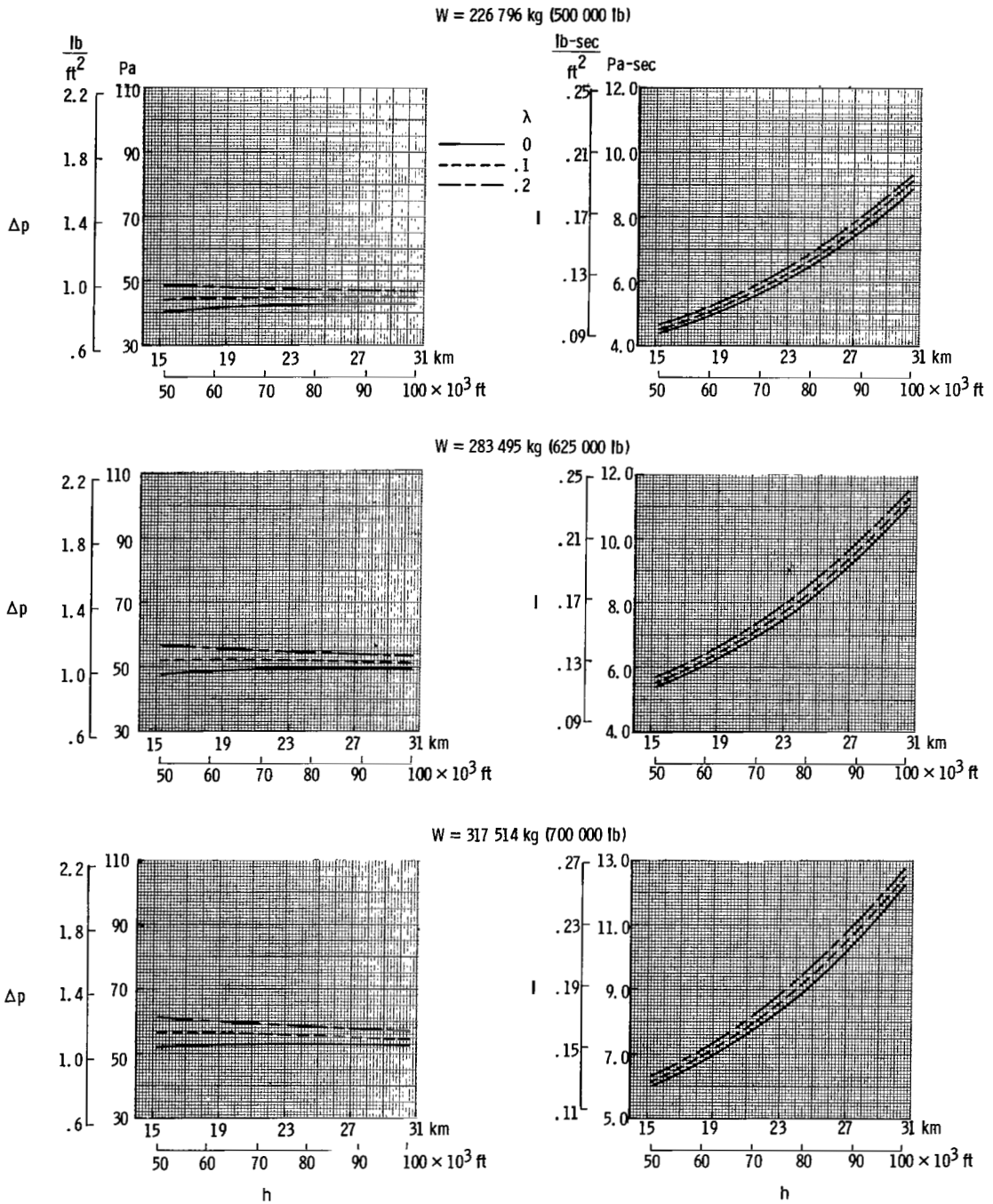


$h = 30,48 \text{ km (100 000 ft)}$



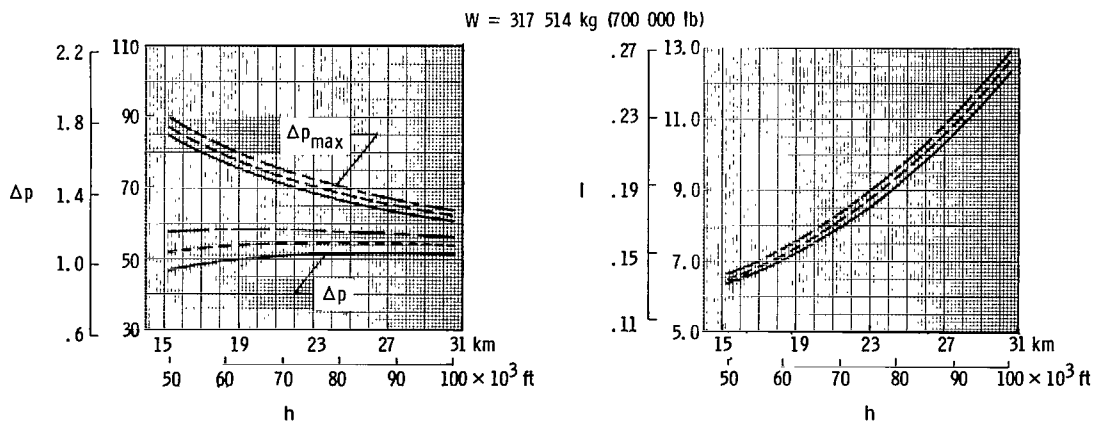
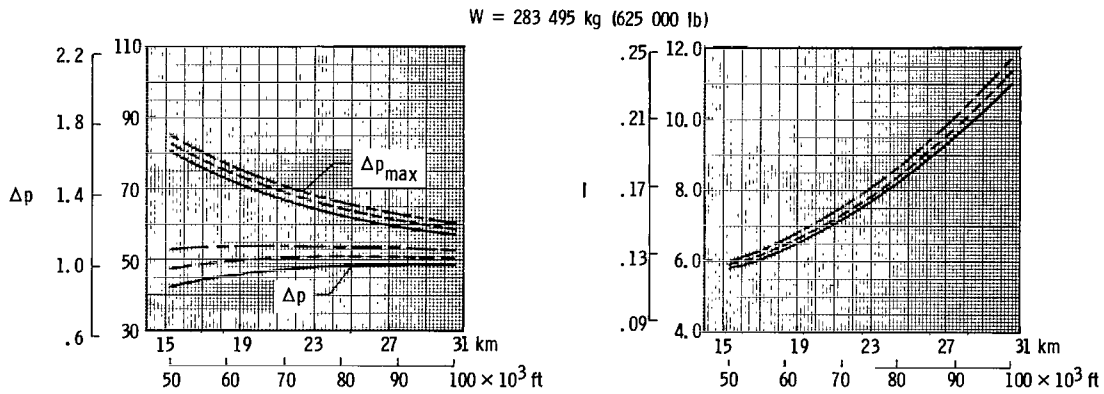
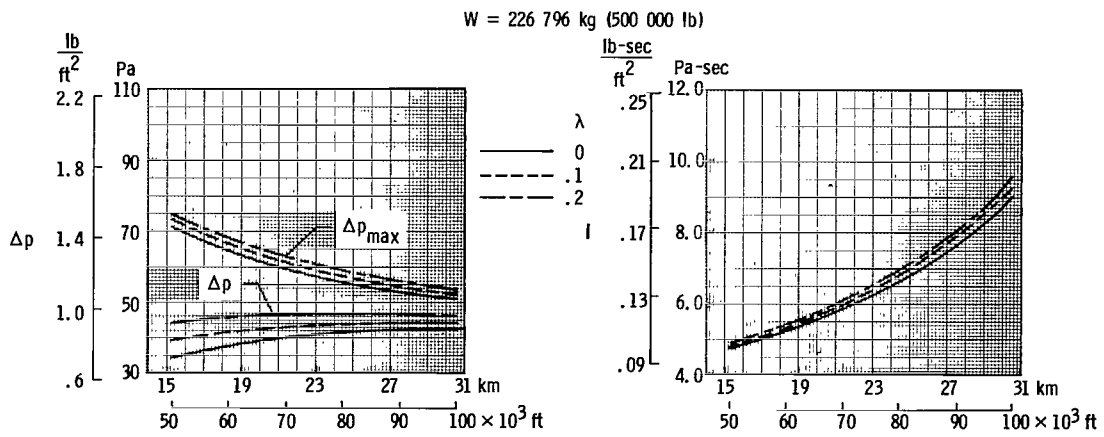
(c) Minimum-shock signature. $\eta = 0.9$.

Figure 7.- Concluded.



(a) "Flat-top" signature.

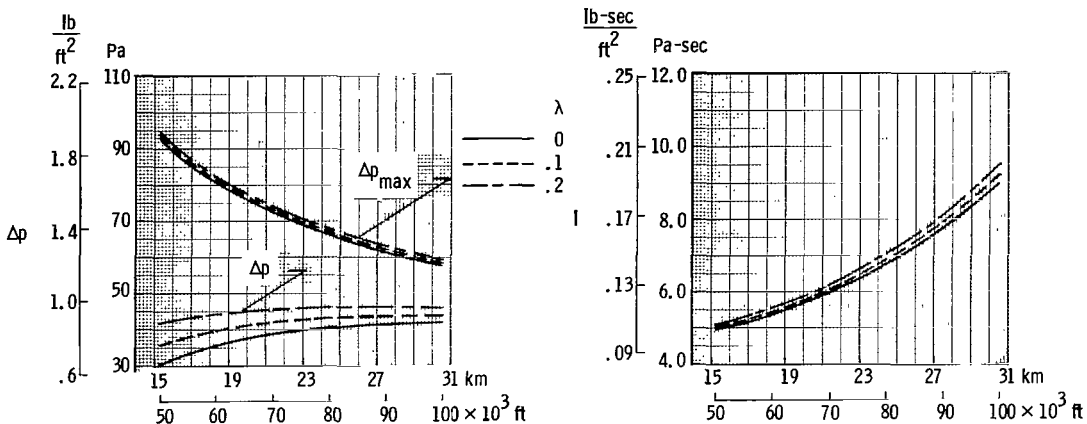
Figure 8.- Variation of overpressure and impulse with altitude. $M = 3.2$; $k = 2.0$; $l = 94.49\text{ m}$ (310 ft).



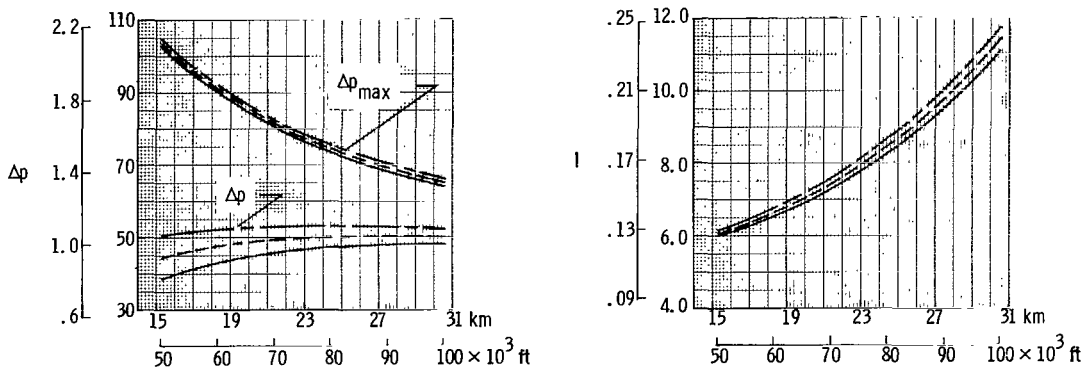
(b) Minimum-shock signature. $\eta = 0.5$.

Figure 8.- Continued.

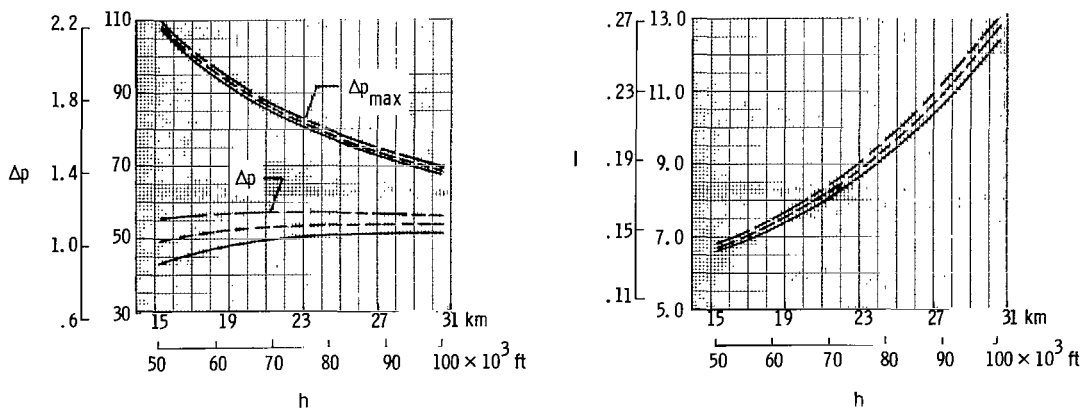
W = 226 796 kg (500 000 lb)



W = 283 495 kg (625 000 lb)

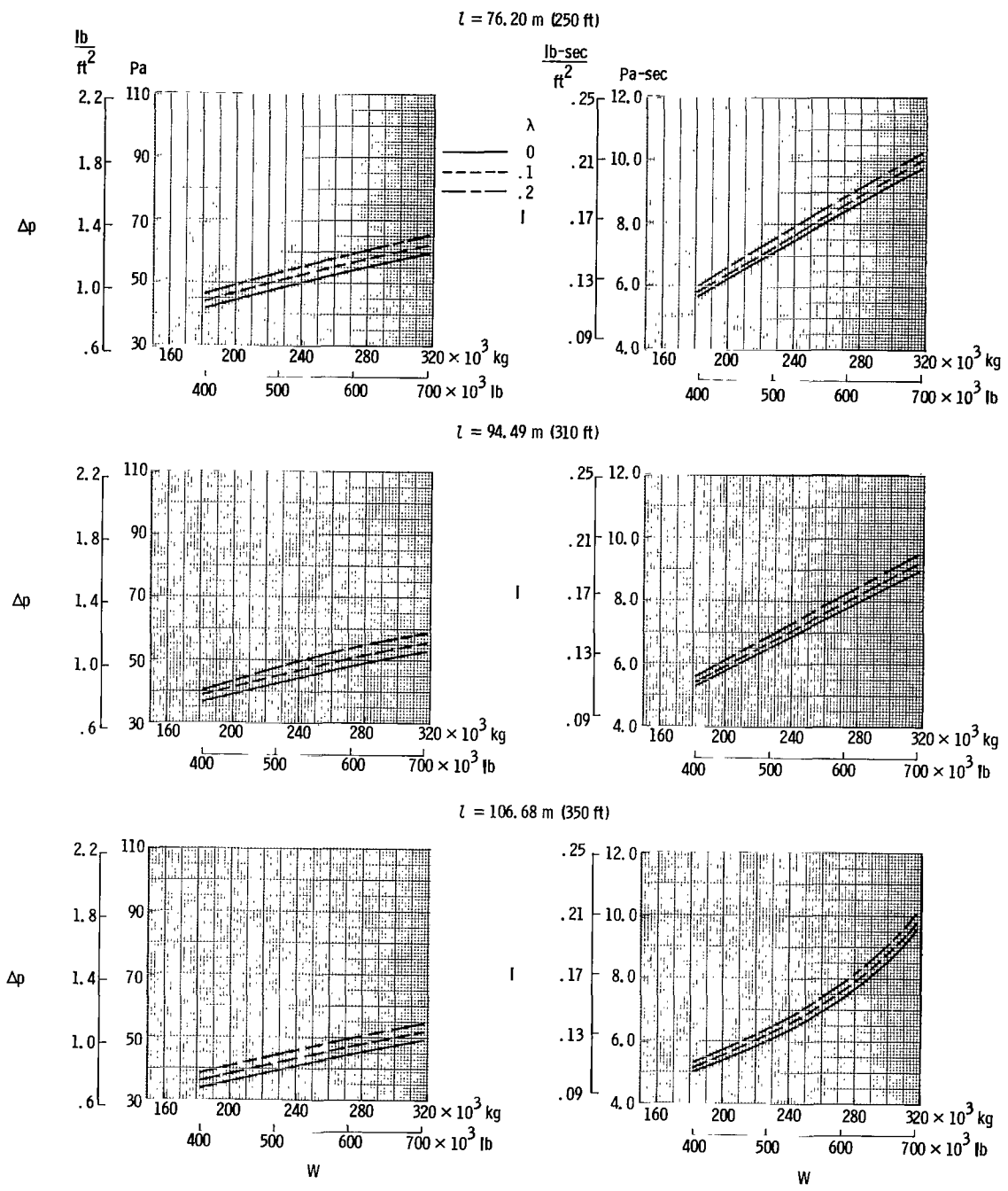


W = 317 514 kg (700 000 lb)



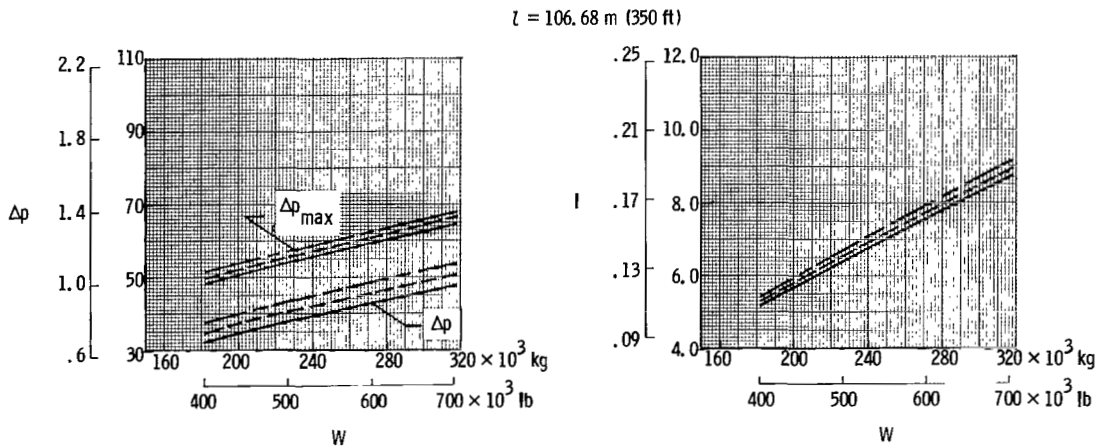
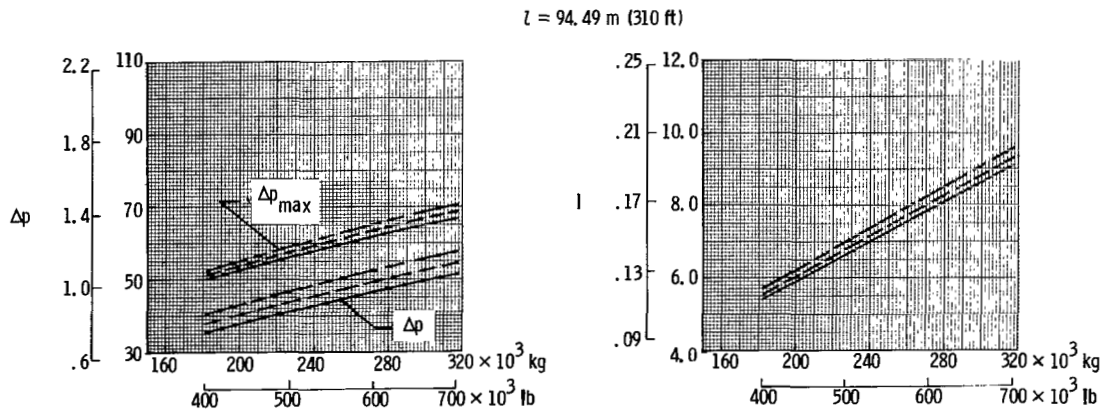
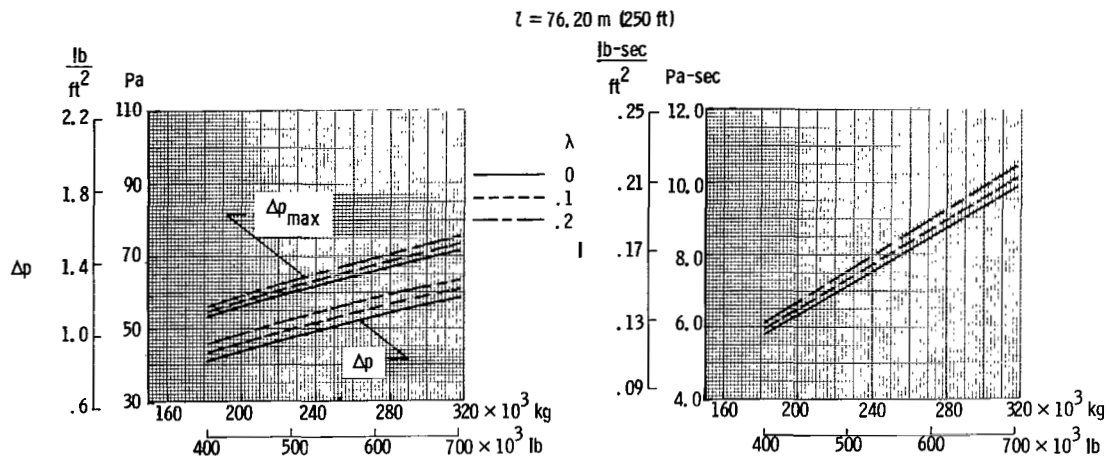
(c) Minimum-shock signature. $\eta = 0.9$.

Figure 8.- Concluded.



(a) "Flat-top" signature.

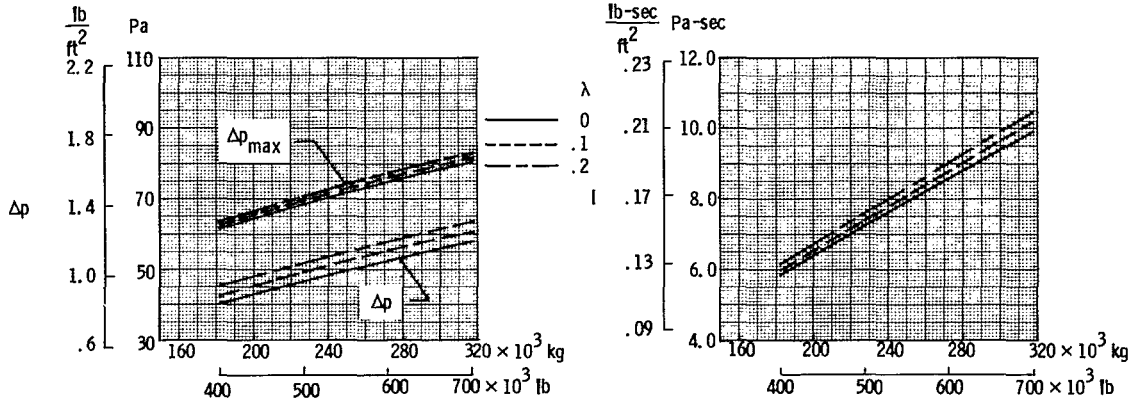
Figure 9.- Variation of overpressure and impulse with weight. $M = 3.2$;
 $k = 2.0$; $h = 24.384 \text{ km (80 000 ft)}$.



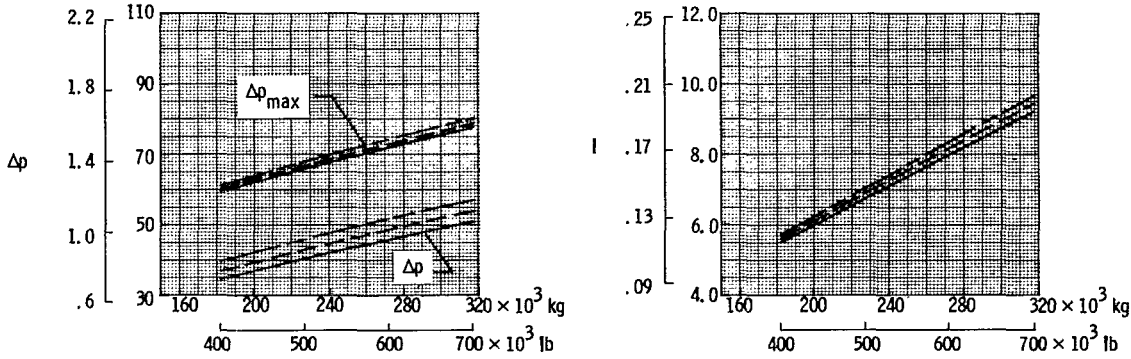
(b) Minimum-shock signature. $\eta = 0.5$.

Figure 9.- Continued.

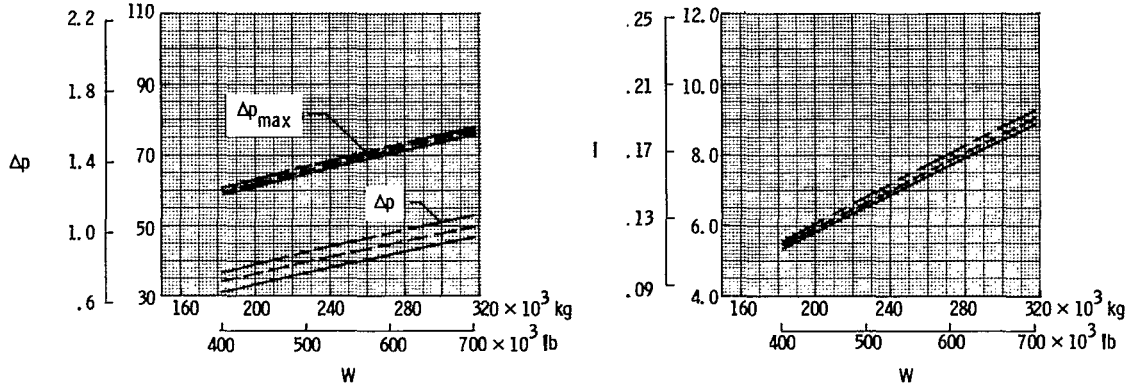
$l = 76.20 \text{ m (250 ft)}$



$l = 94.49 \text{ m (310 ft)}$



$l = 106.68 \text{ m (350 ft)}$



(c) Minimum-shock signature. $\eta = 0.9$.

Figure 9.- Concluded.

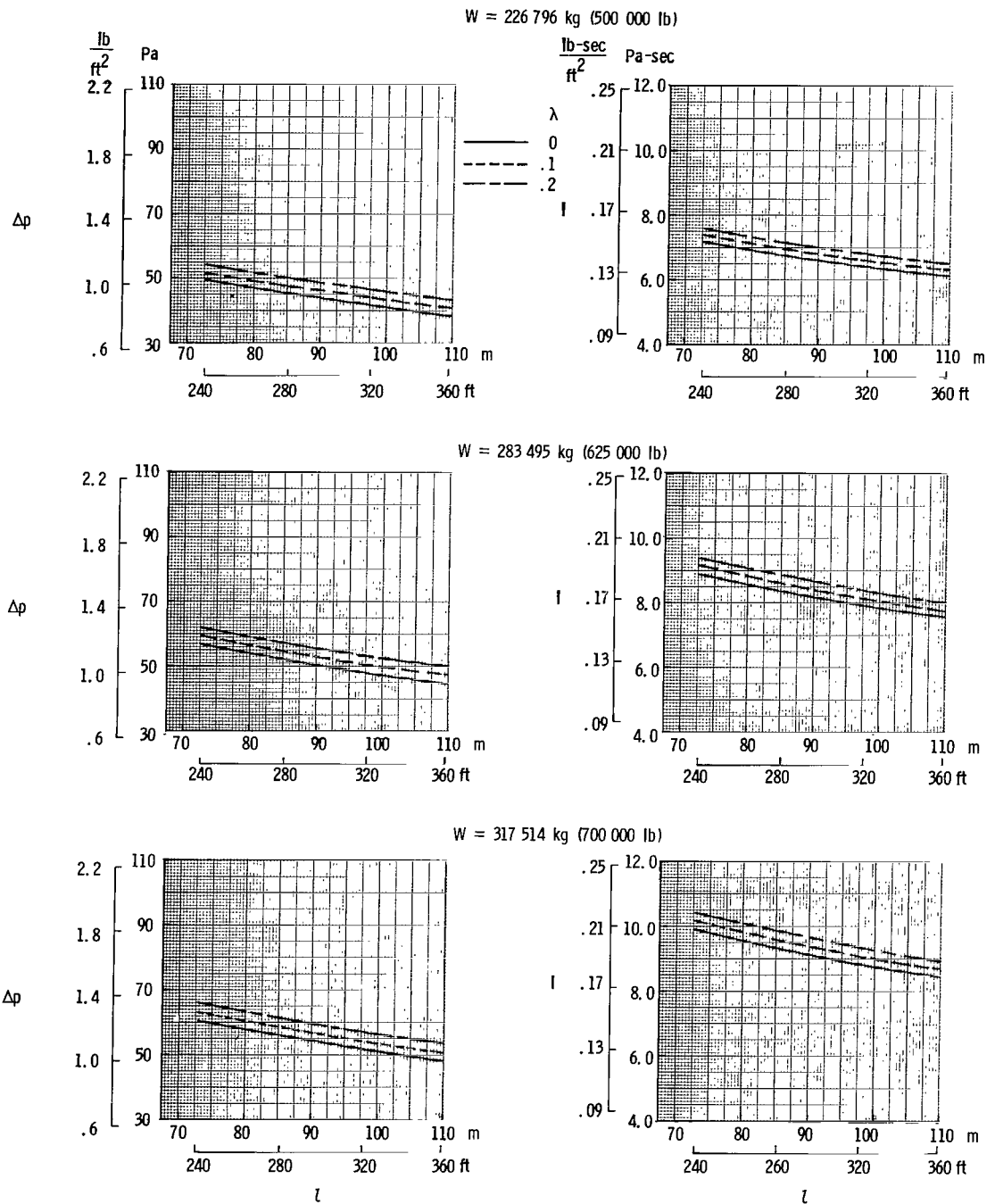
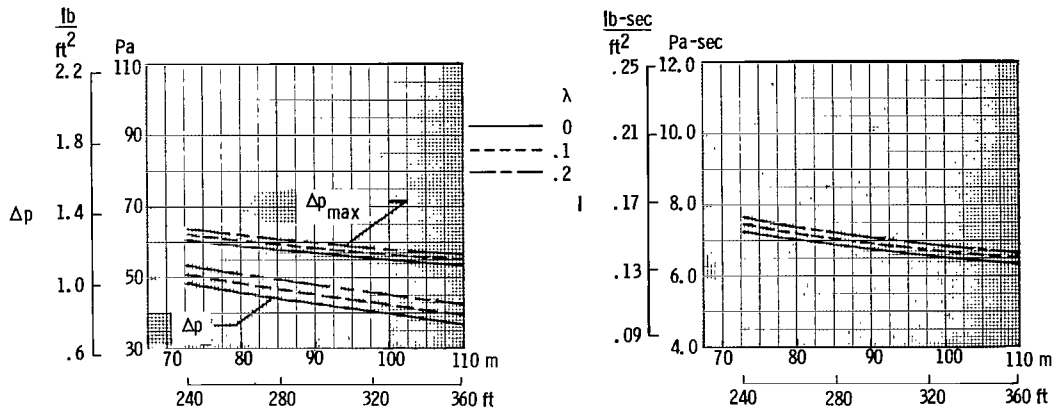
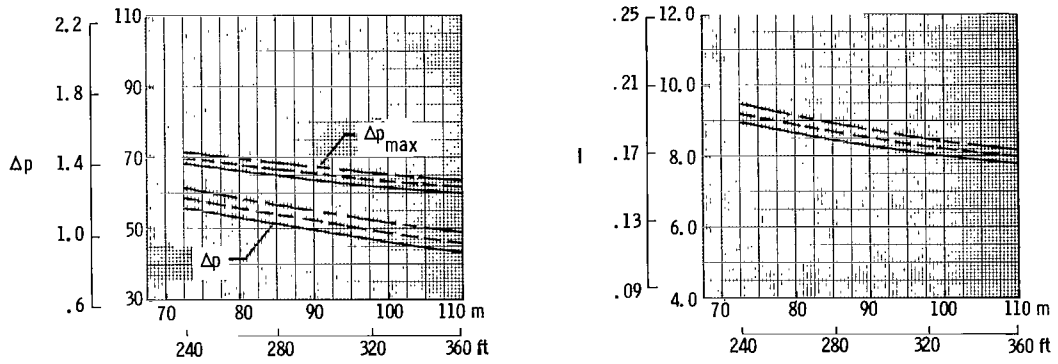


Figure 10.- Variation of overpressure and impulse with length. $M = 3.2$;
 $k = 2.0$; $h = 24.384 \text{ km (80\,000 ft)}$.

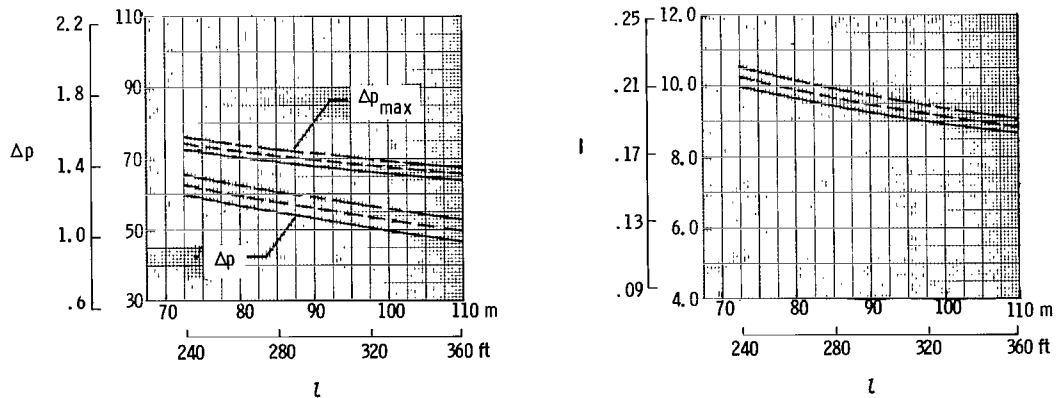
W = 226 796 kg (500 000 lb)



W = 283 495 kg (625 000 lb)

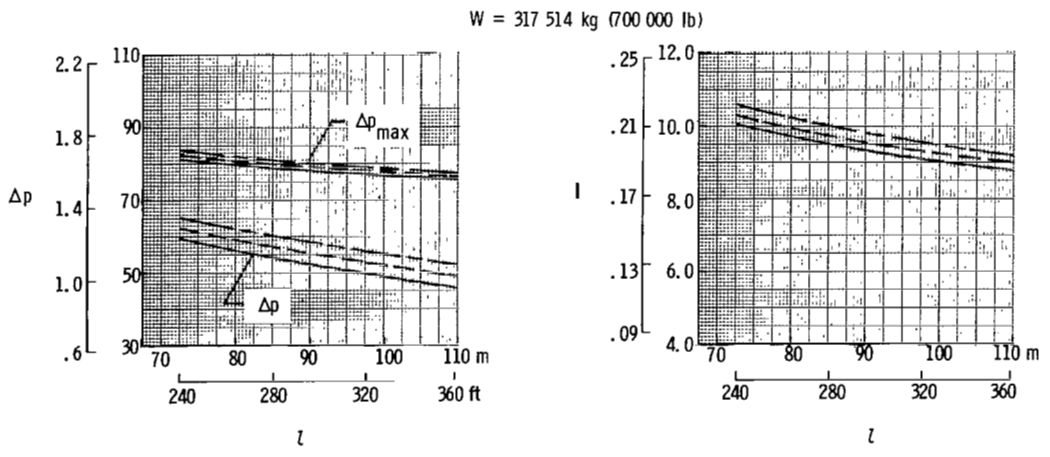
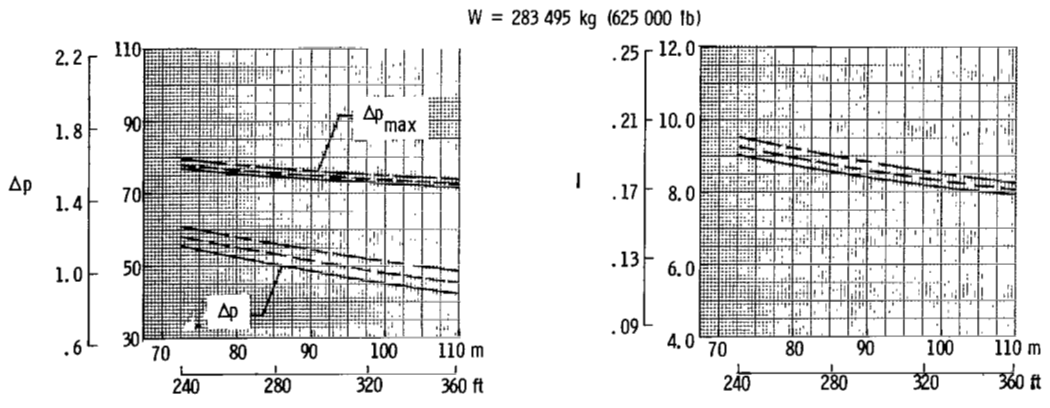
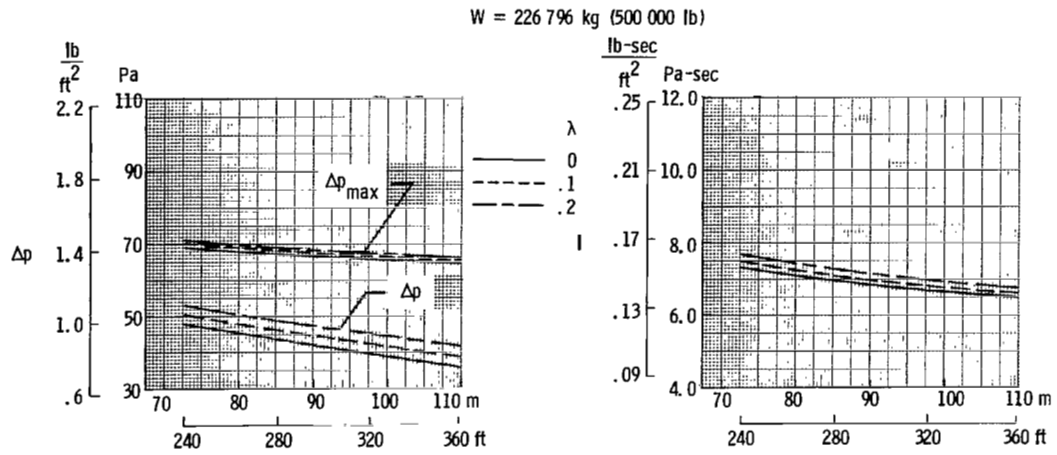


W = 317 514 kg (700 000 lb)



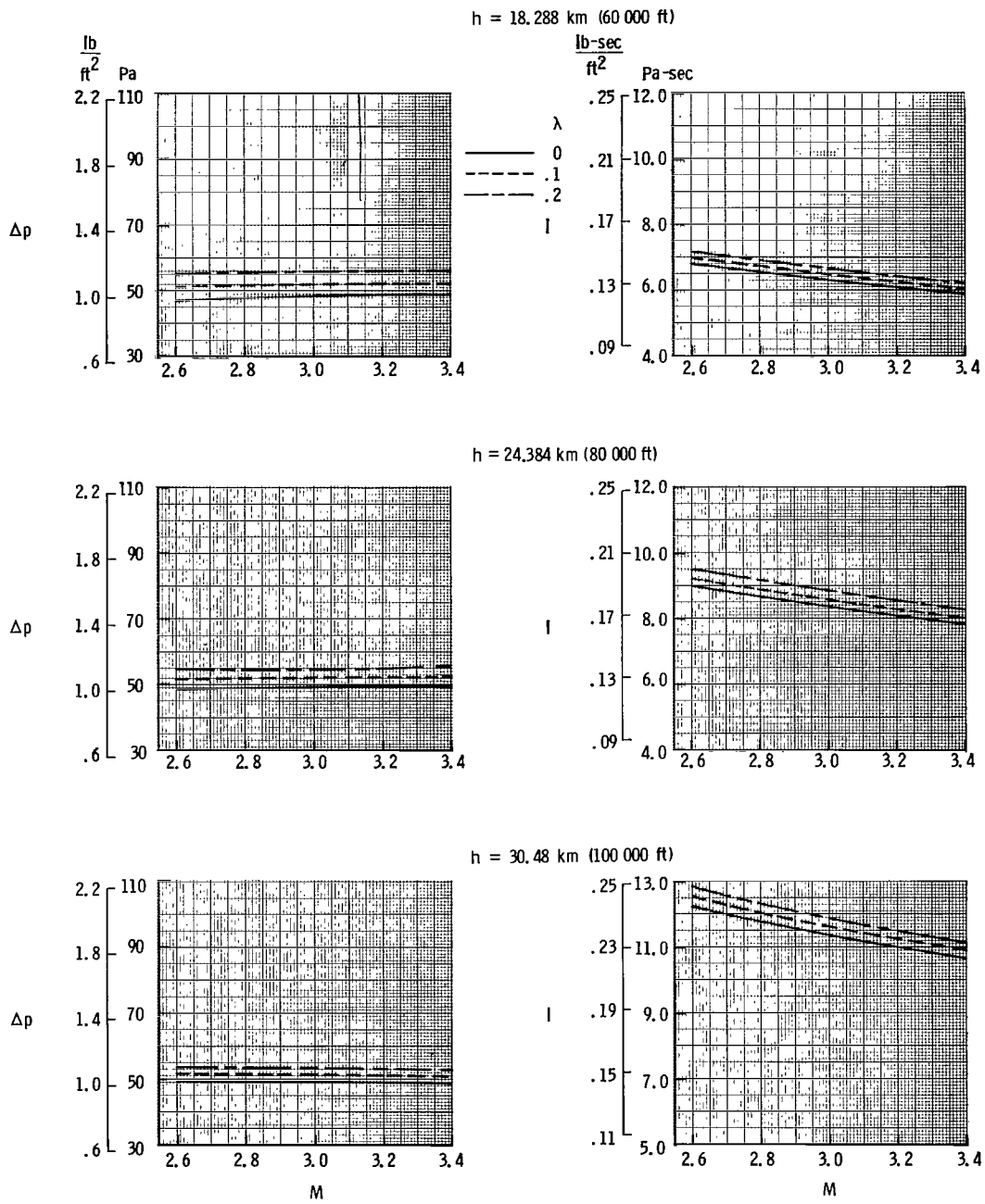
(b) Minimum-shock signature. $\eta = 0.5$.

Figure 10.- Continued.



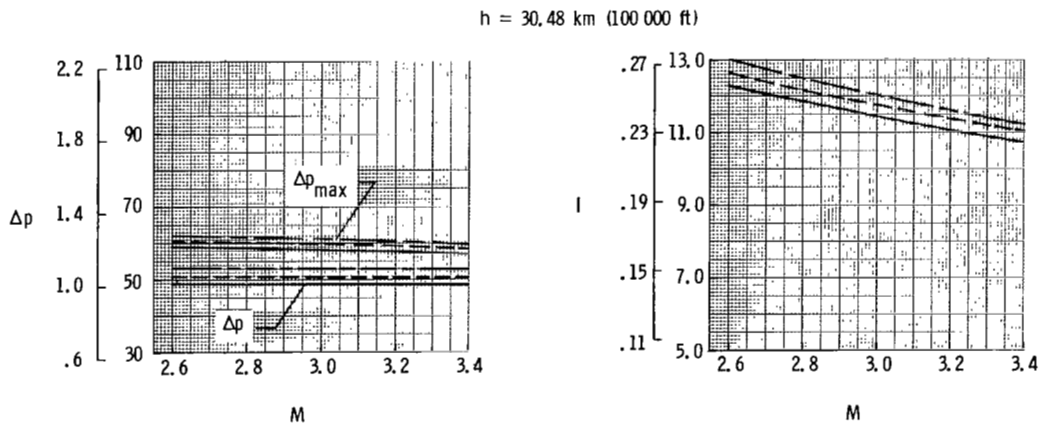
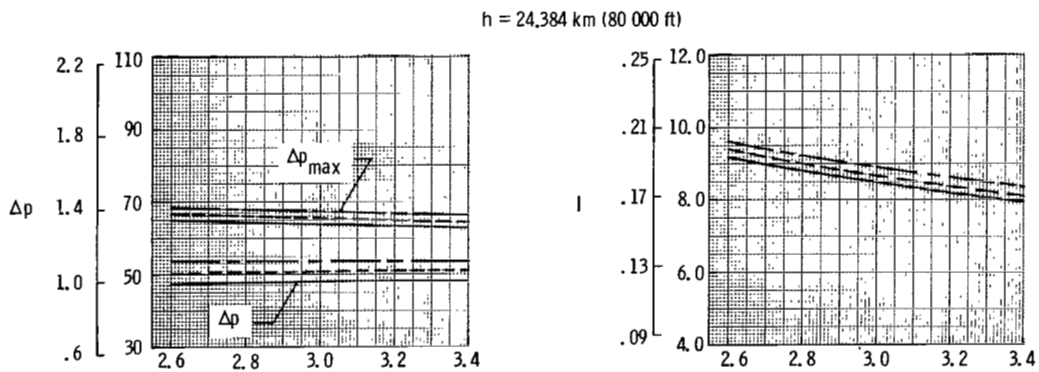
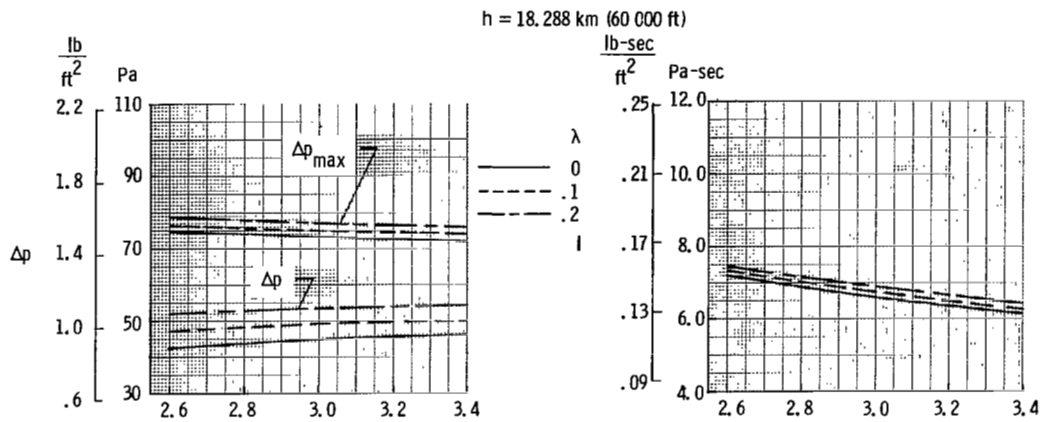
(c) Minimum-shock signature. $\eta = 0.9$.

Figure 10.- Concluded.



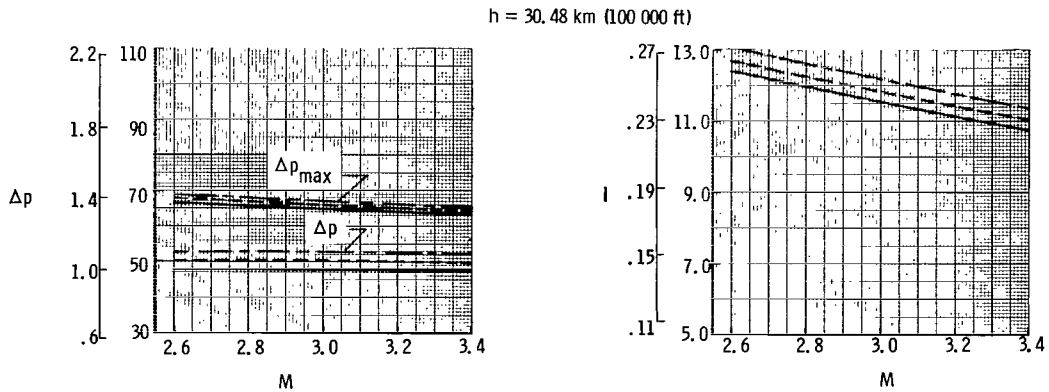
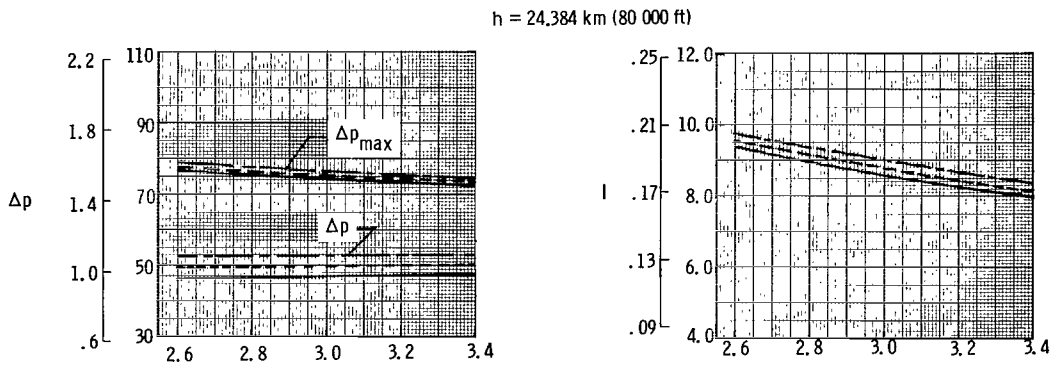
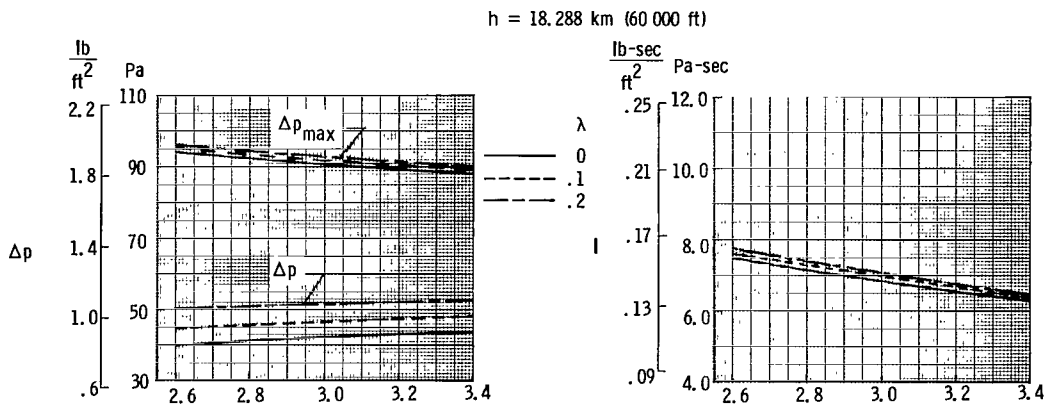
(a) "Flat-top" signature.

Figure 11.- Variation of overpressure and impulse with Mach number. $k = 2.0$;
 $\zeta = 94.49 \text{ m (310 ft)}$; $W = 283\,495 \text{ kg (625\,000 lb)}$.



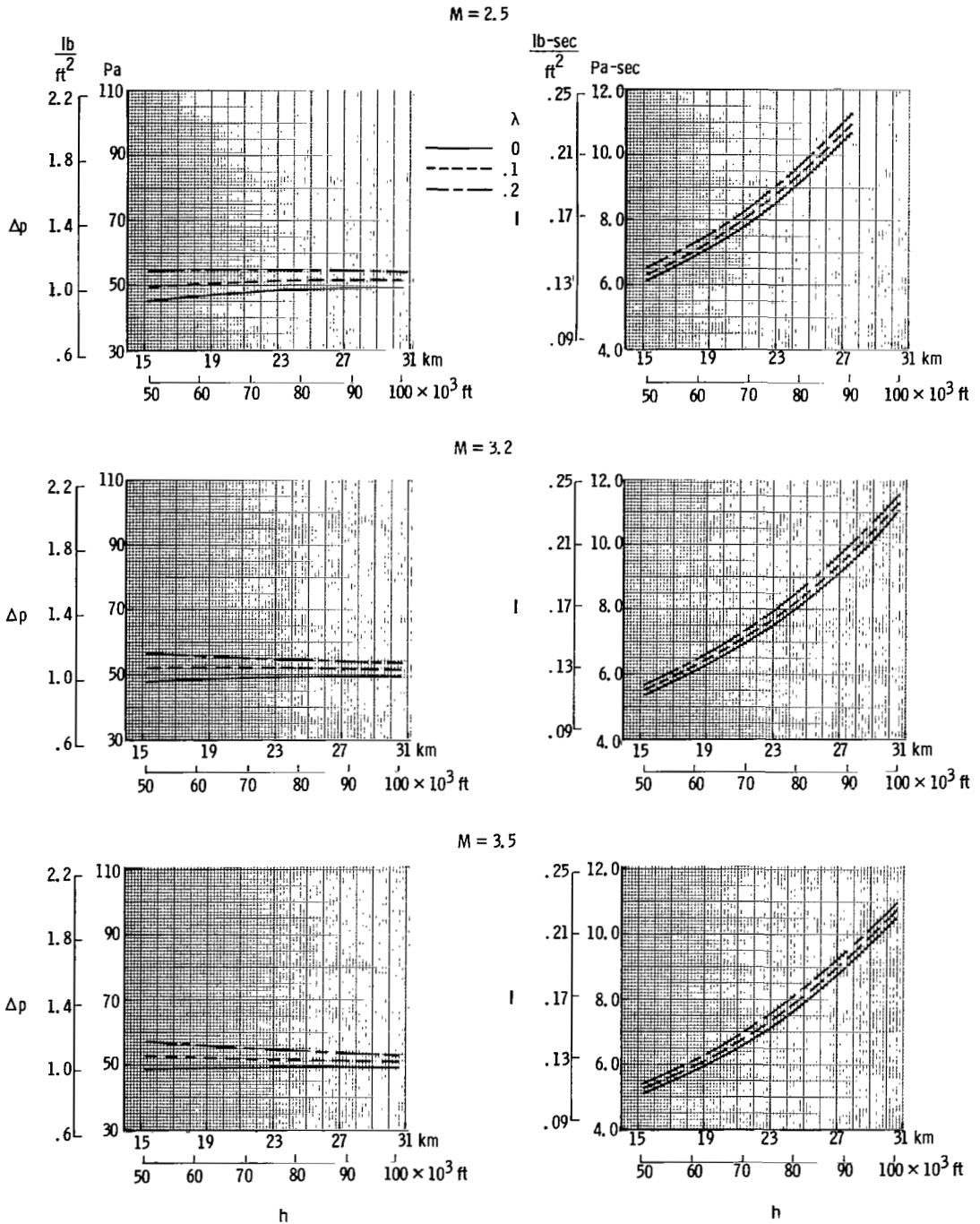
(b) Minimum-shock signature. $\eta = 0.5$.

Figure 11.- Continued.



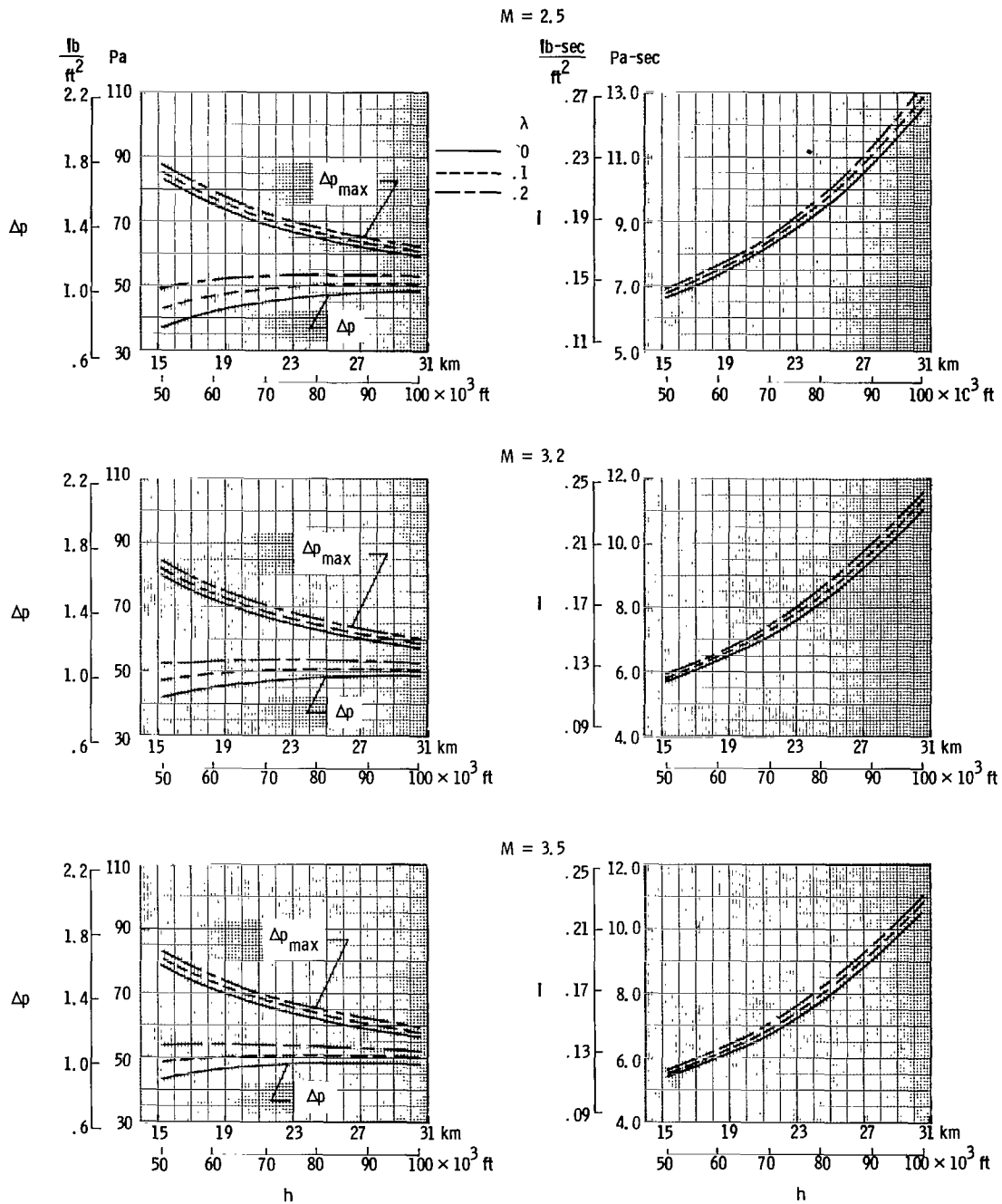
(c) Minimum-shock signature. $\eta = 0.9$.

Figure 11.- Concluded.



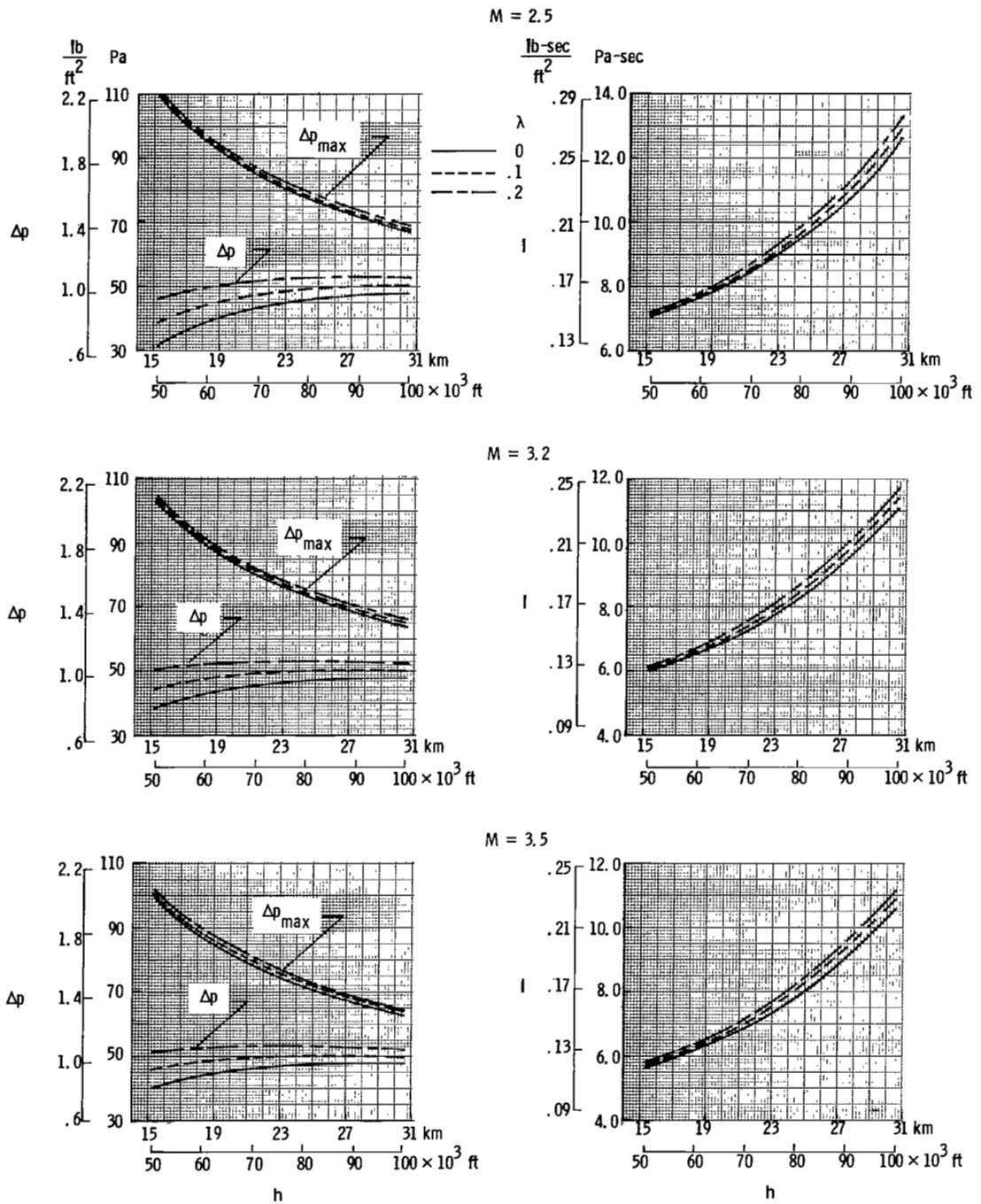
(a) "Flat-top" signature.

Figure 12.- Variation of overpressure and impulse with altitude. $k = 2.0$;
 $l = 94.49 \text{ m (310 ft)}$; $W = 283\,495 \text{ kg (625\,000 lb)}$.



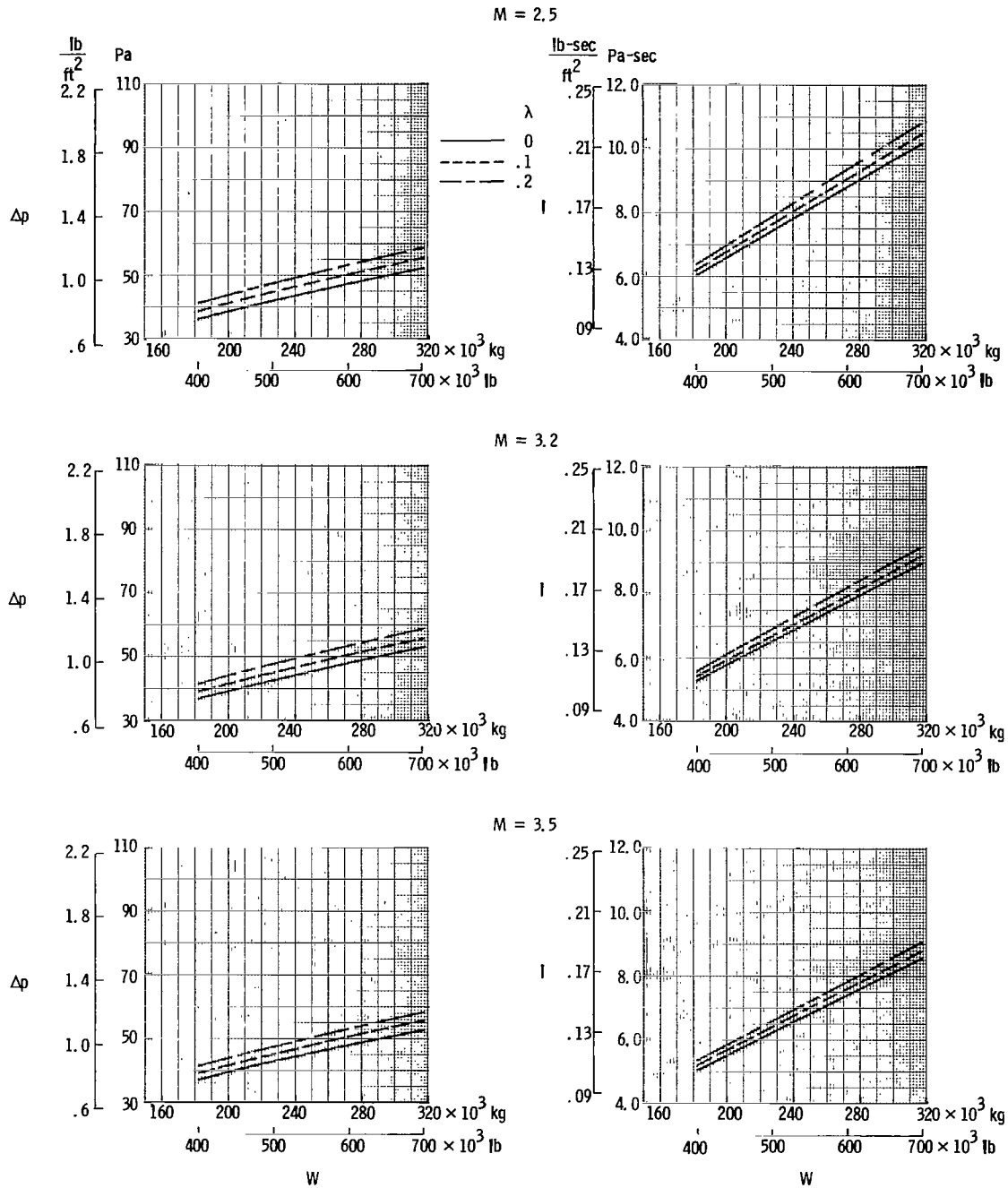
(b) Minimum-shock signature. $\eta = 0.5$.

Figure 12.- Continued.



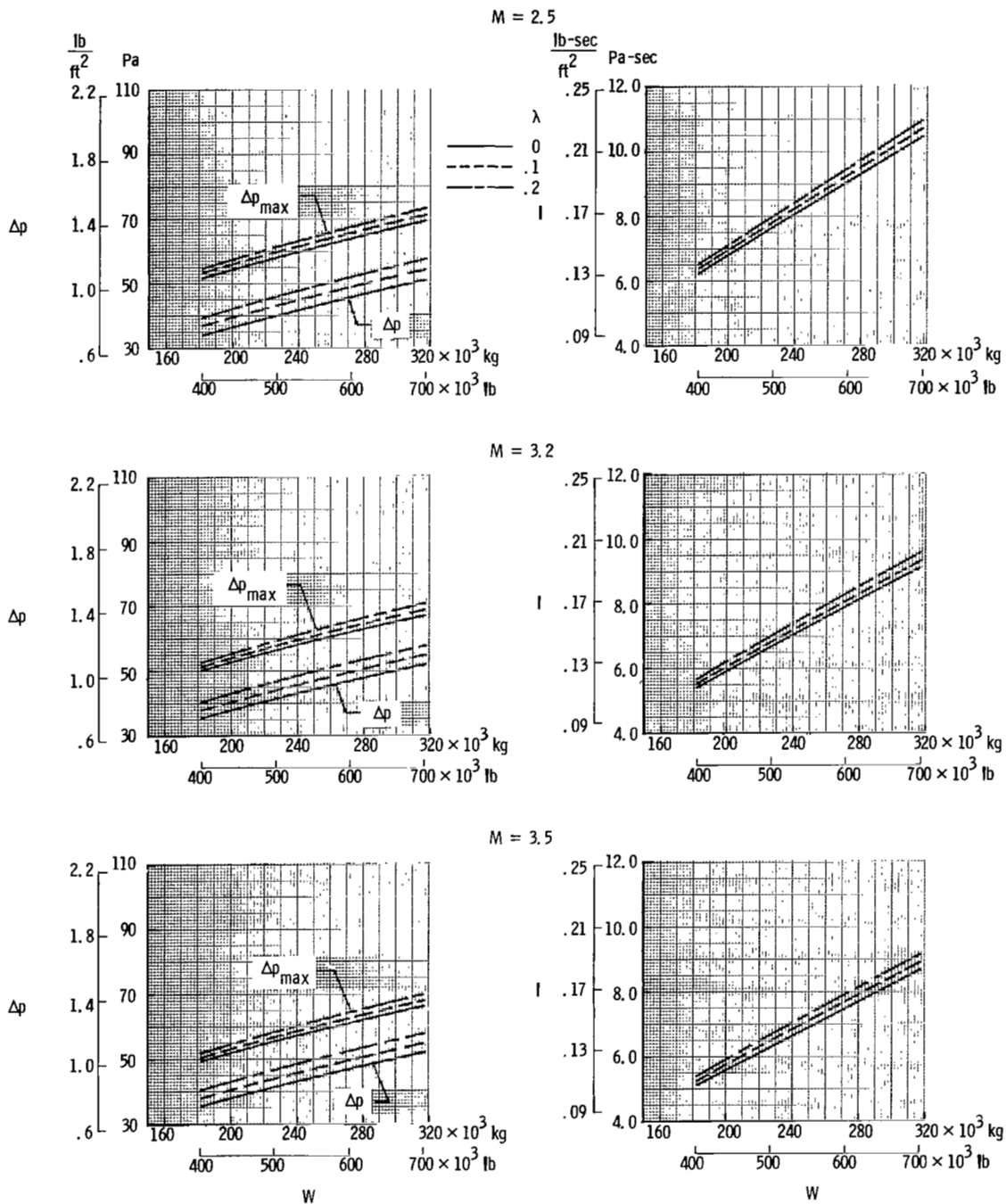
(c) Minimum-shock signature. $\eta = 0.9$.

Figure 12.- Concluded.



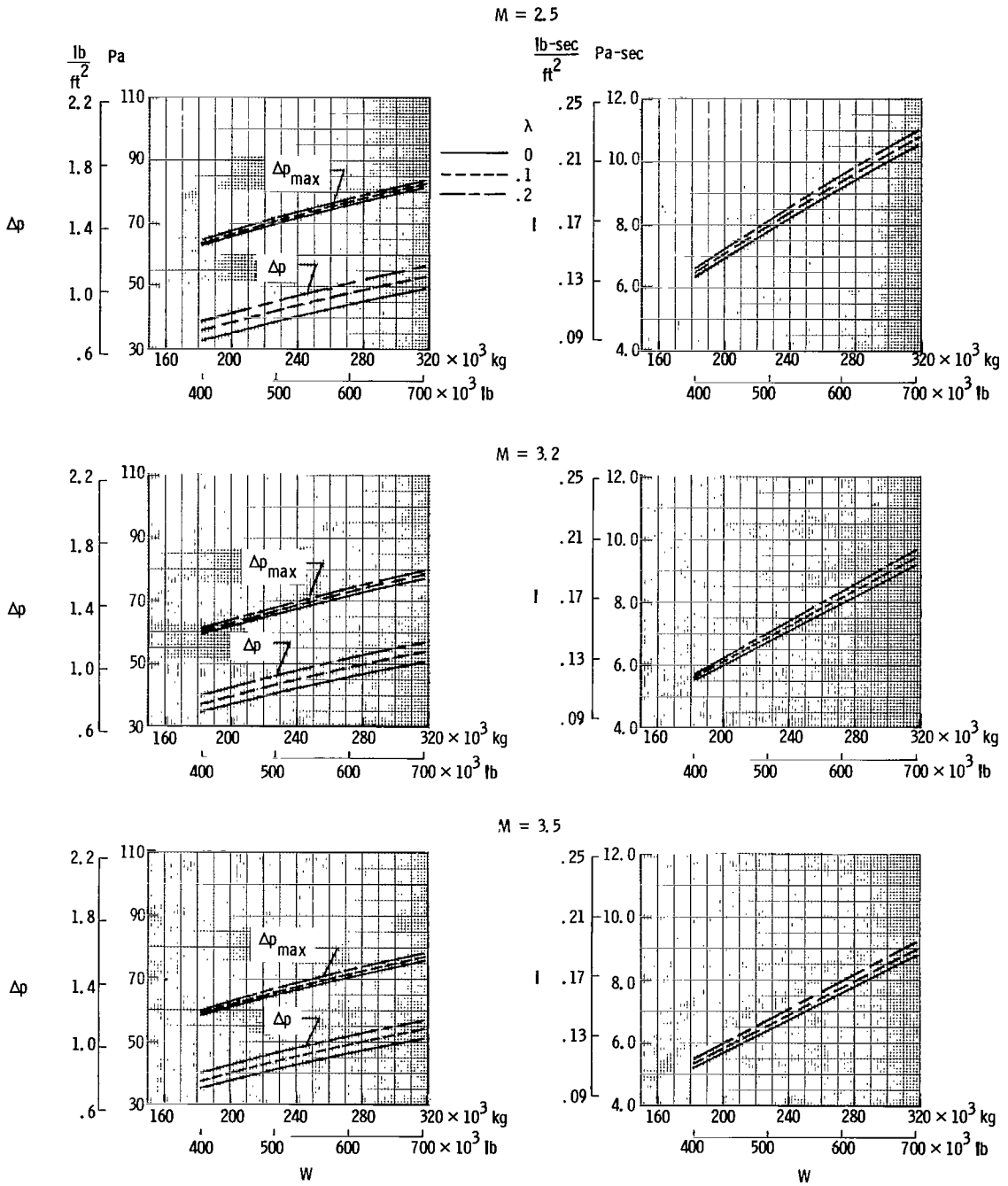
(a) "Flat-top" signature.

Figure 13.- Variation of overpressure and impulse with weight. $k = 2.0$;
 $z = 94.49$ m (310 ft); $h = 24.384$ km (80 000 ft).



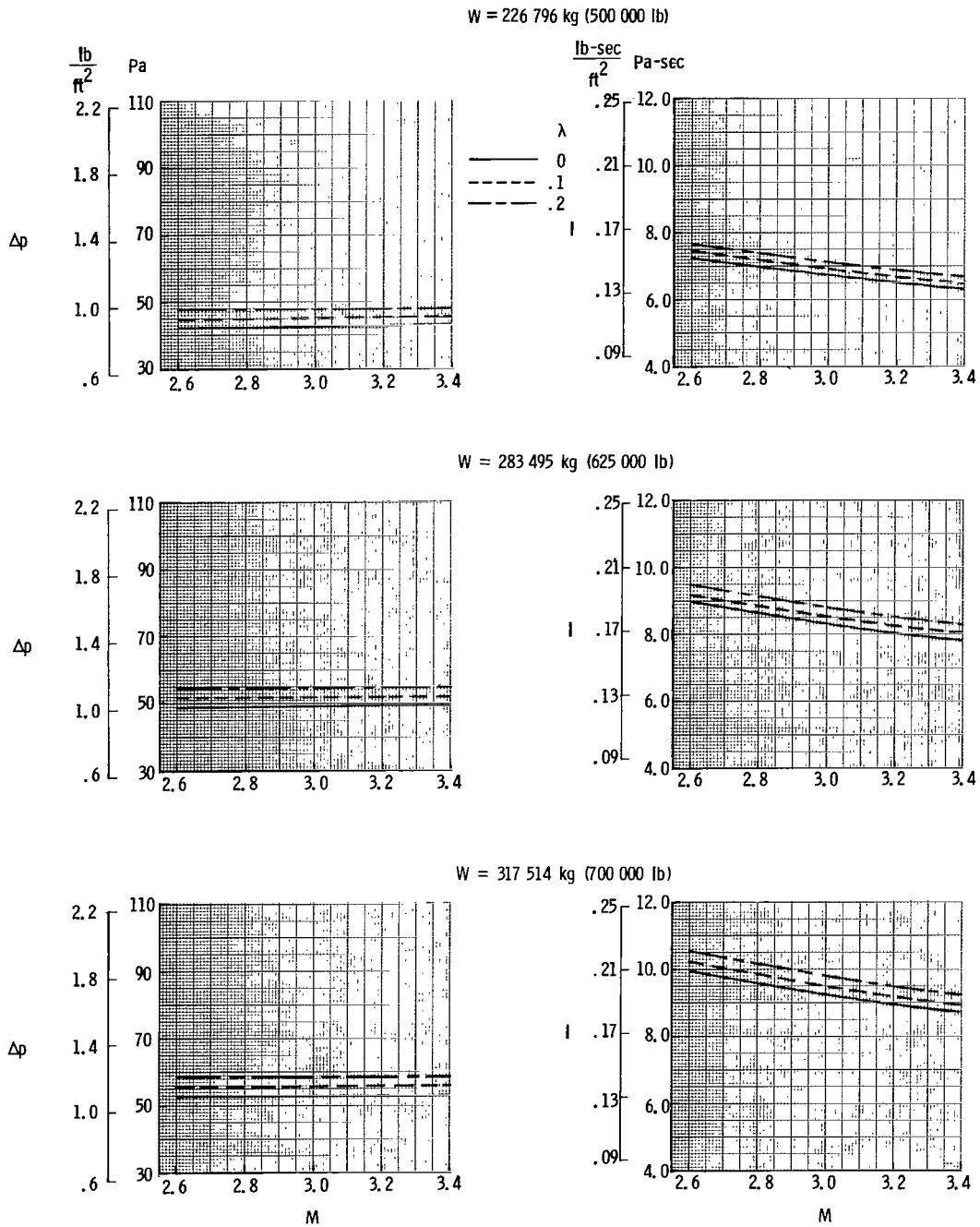
(b) Minimum-shock signature. $\eta = 0.5$.

Figure 13.- Continued.



(c) Minimum-shock signature. $\eta = 0.9$.

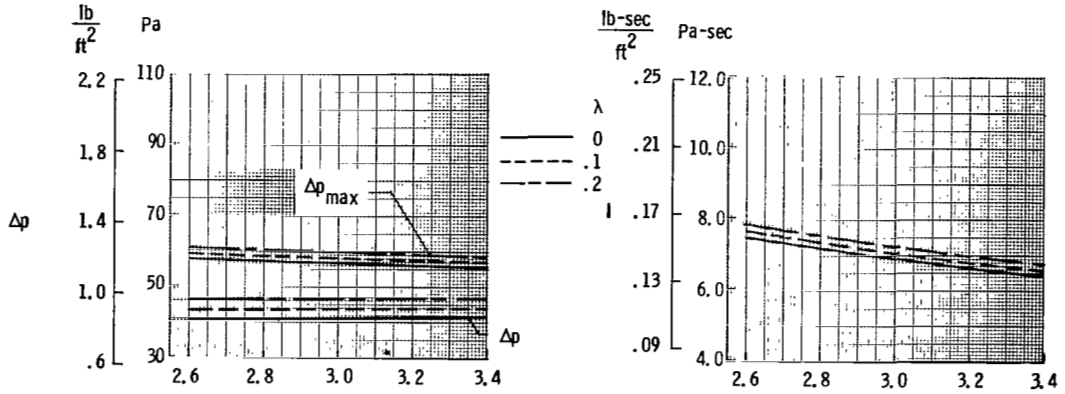
Figure 13.- Concluded.



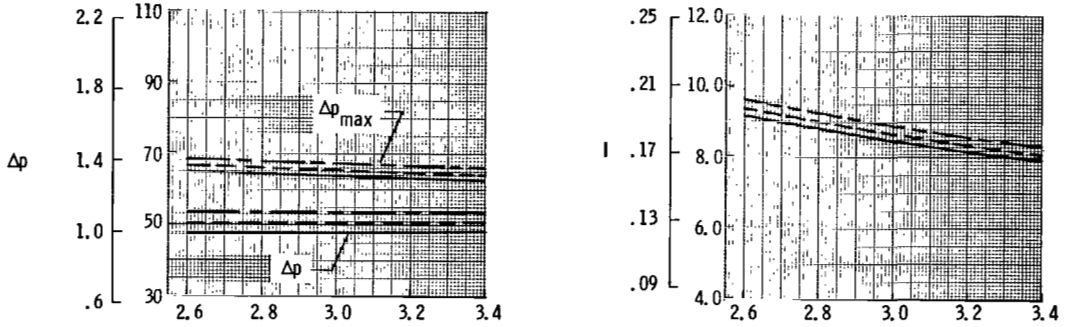
(a) "Flat-top" signature.

Figure 14.- Variation of overpressure and impulse with Mach number.
 $k = 2.0$; $l = 94.49 \text{ m (310 ft)}$; $h = 24.384 \text{ km (80 000 ft)}$.

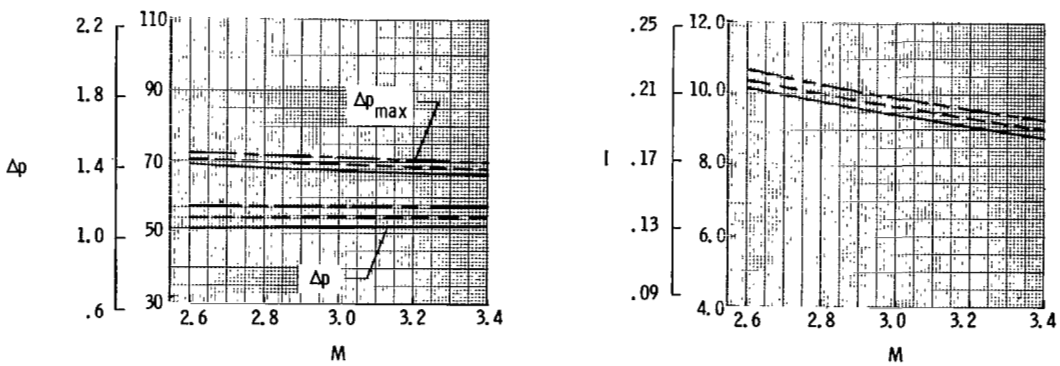
W = 226 796 kg (500 000 lb)



W = 283 495 kg (625 000 lb)

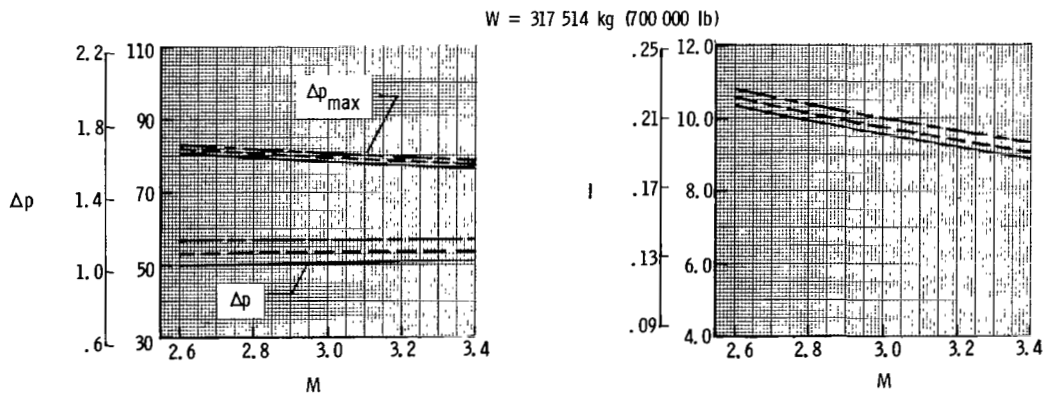
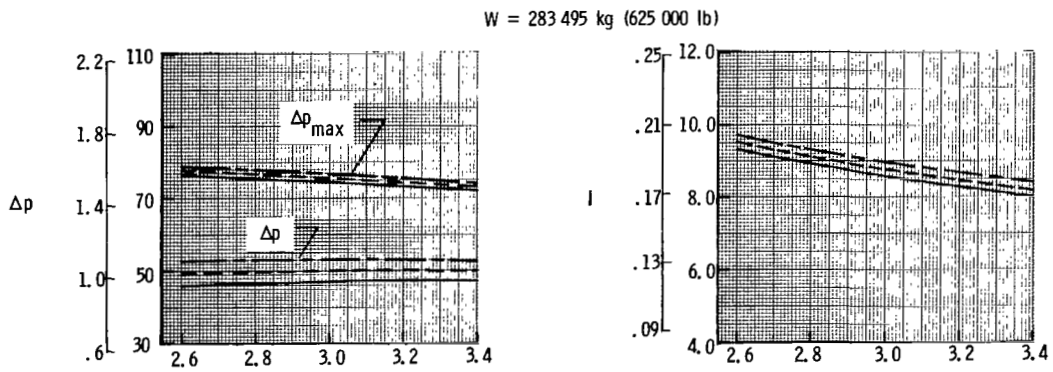
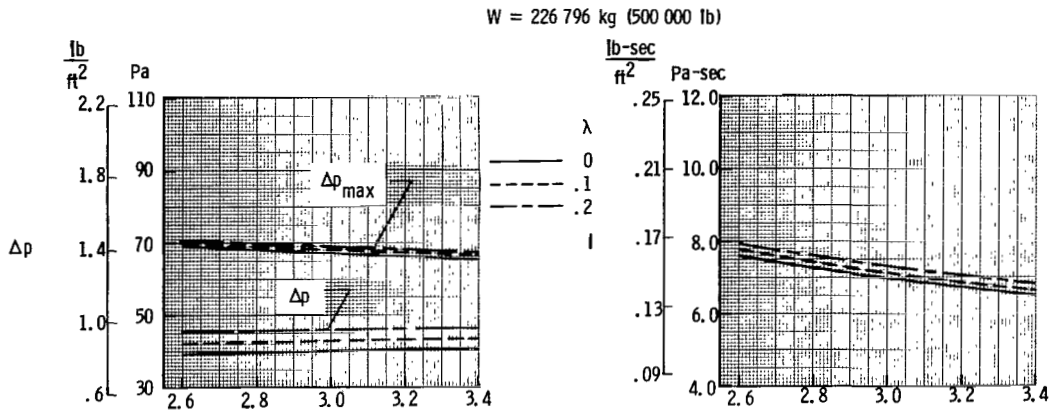


W = 317 514 kg (700 000 lb)



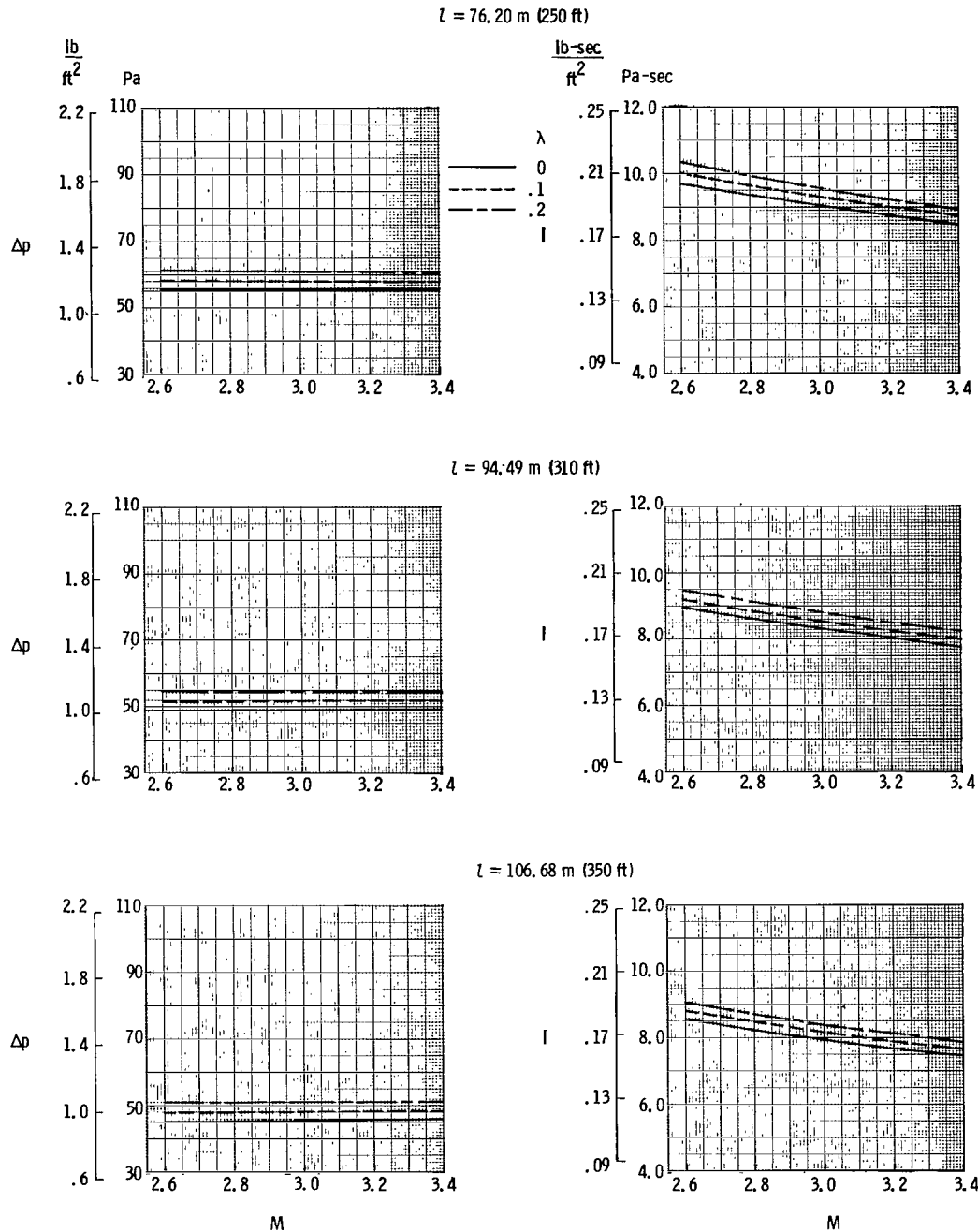
(b) Minimum-shock signature. $\eta = 0.5$.

Figure 14.- Continued.



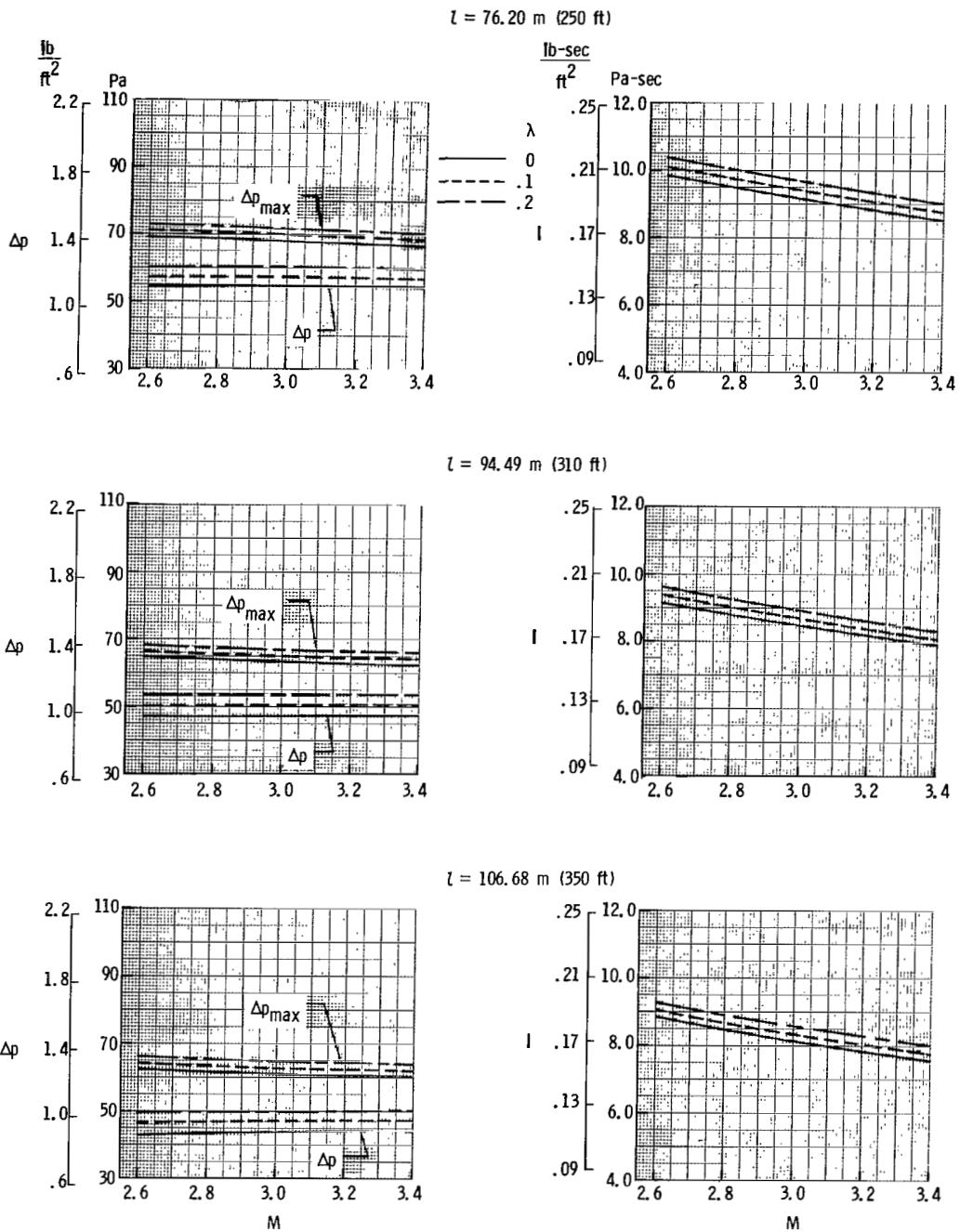
(c) Minimum-shock signature. $\eta = 0.9$.

Figure 14.- Concluded.



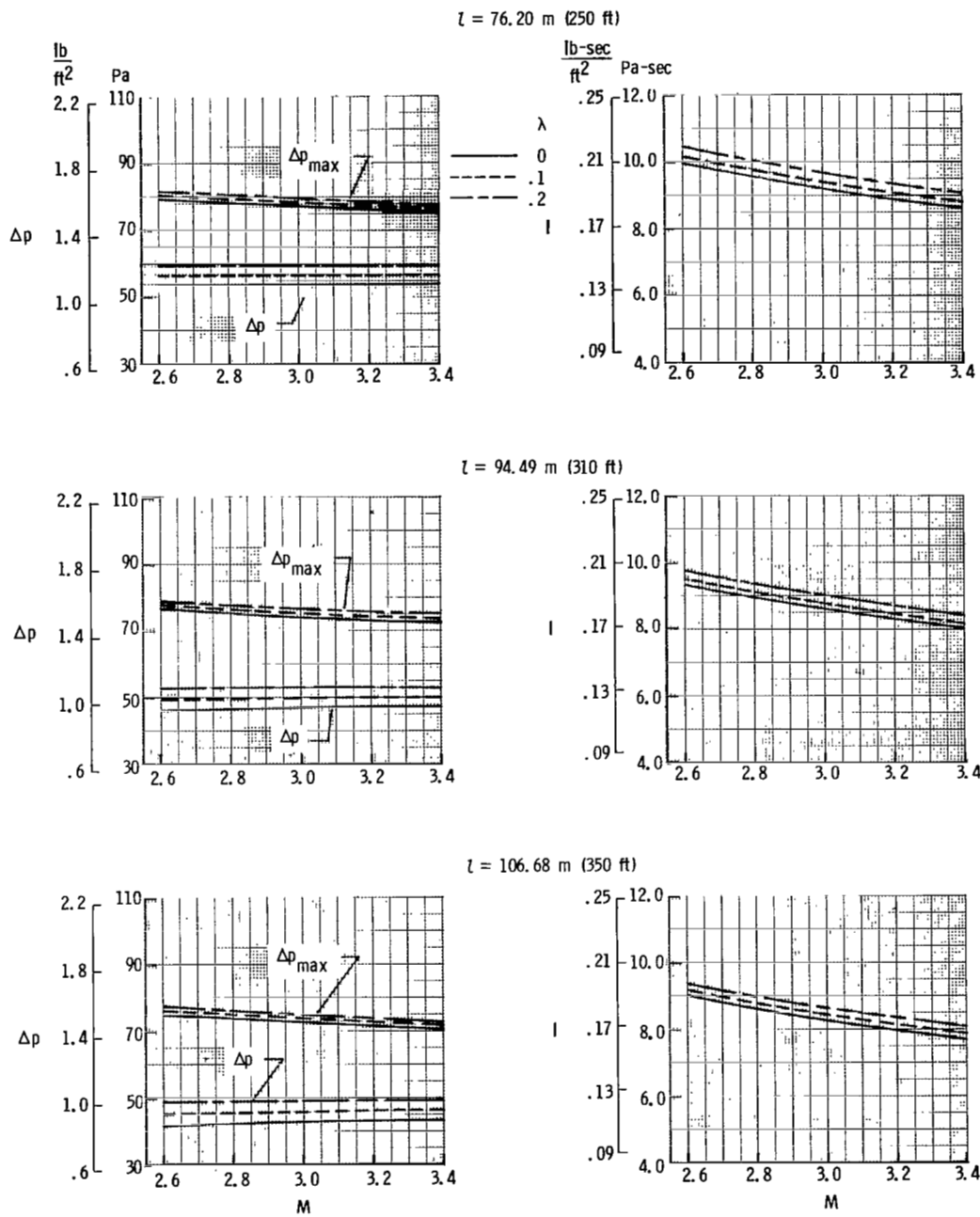
(a) "Flat-top" signature.

Figure 15.- Variation of overpressure and impulse with Mach number. $k = 2.0$;
 $h = 24.384 \text{ km (80 000 ft)}$; $W = 283 495 \text{ kg (625 000 lb)}$.



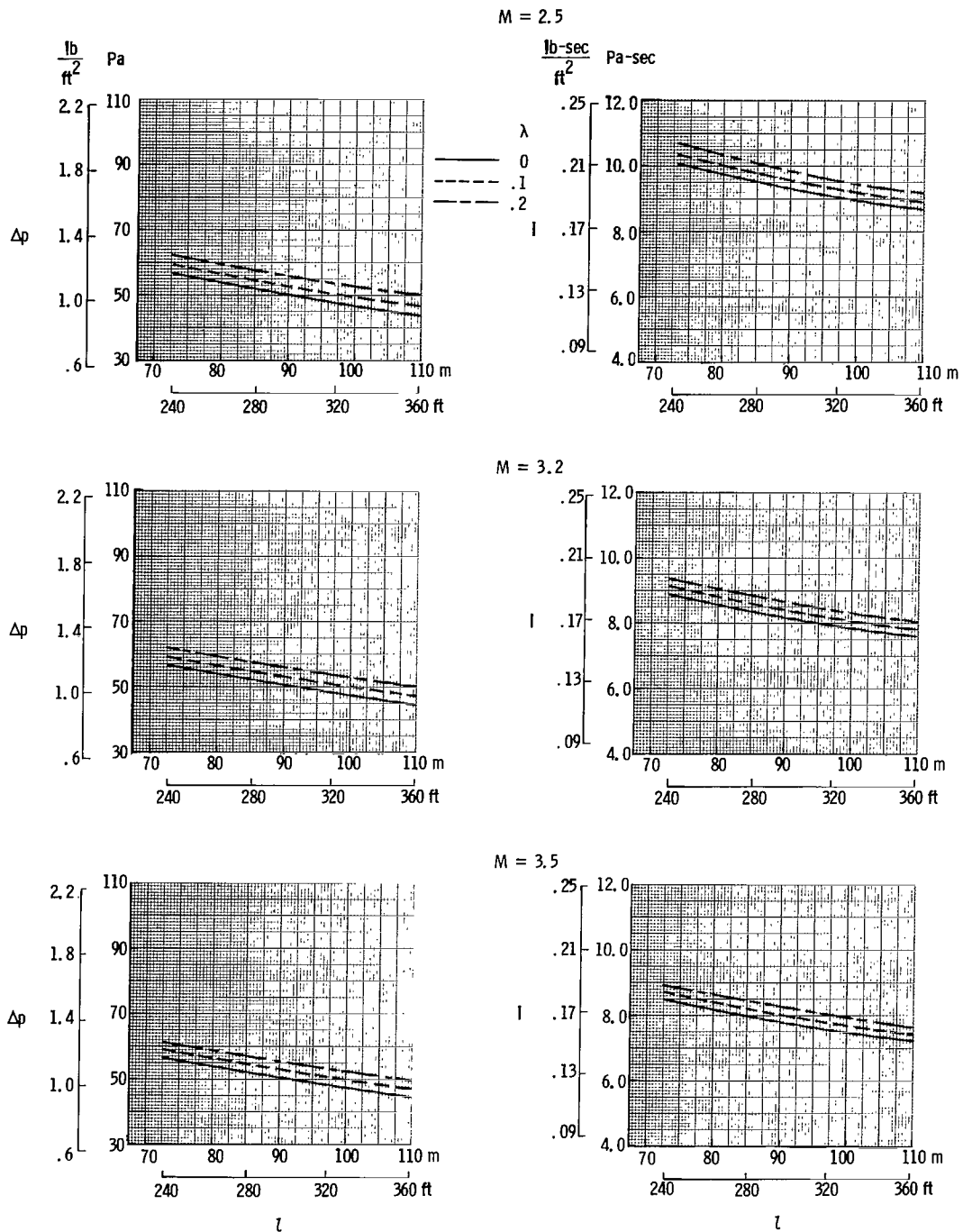
(b) Minimum-shock signature. $\eta = 0.5$.

Figure 15.- Continued.



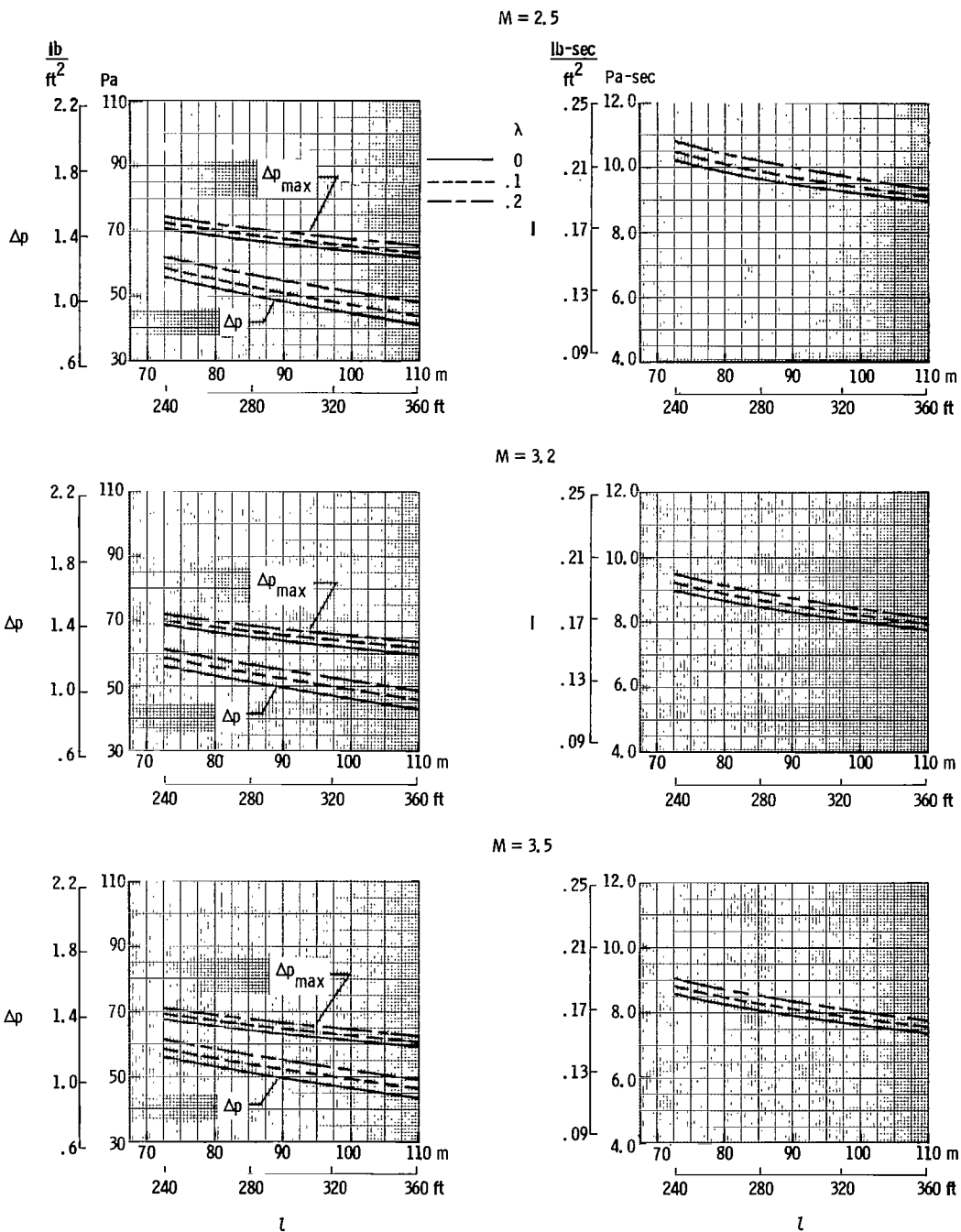
(c) Minimum-shock signature. $\eta = 0.9$.

Figure 15.- Concluded.



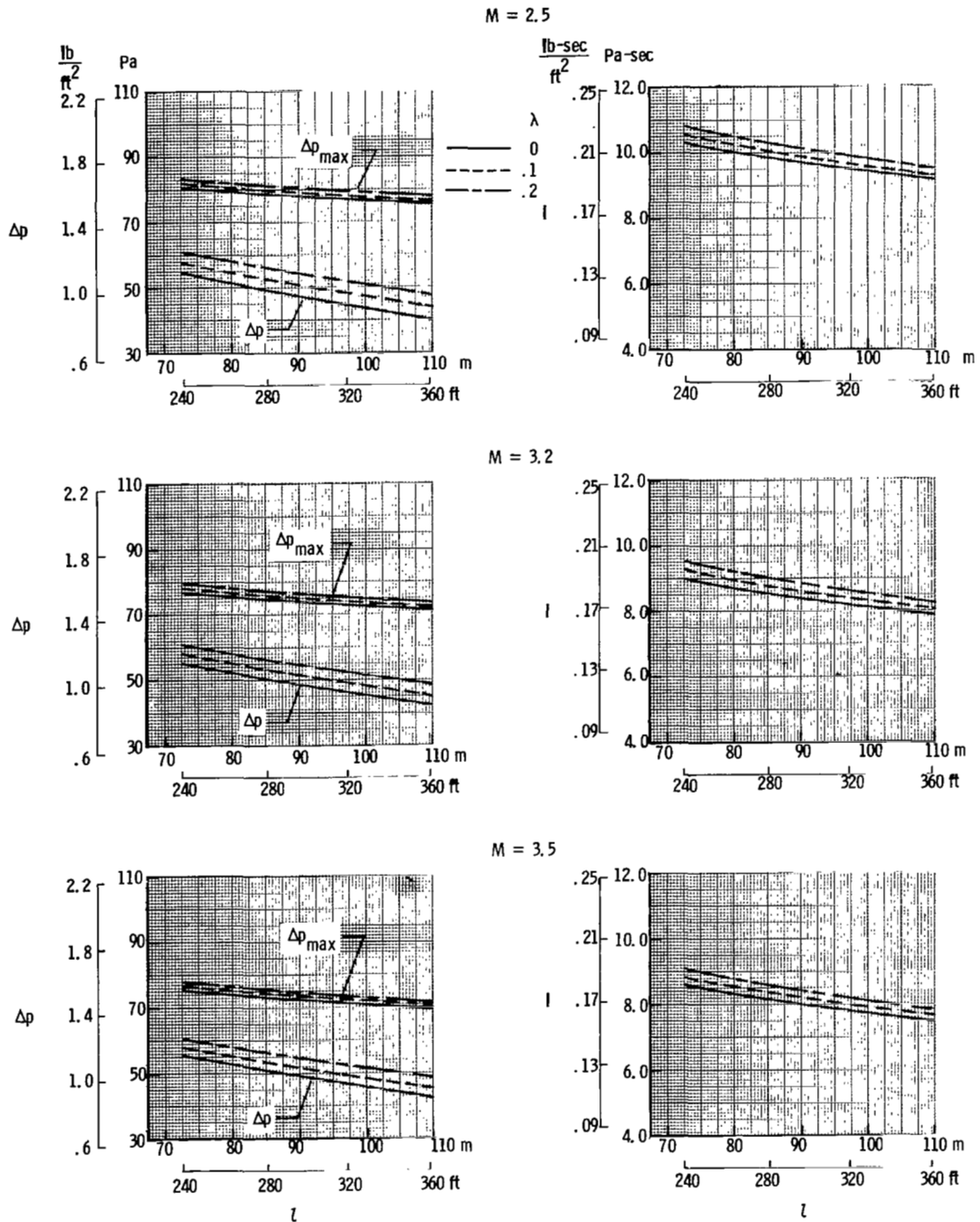
(a) "Flat-top" signature.

Figure 16.- Variation of overpressure and impulse with length. $k = 2.0$;
 $h = 24.384 \text{ km (80 000 ft)}$; $W = 283 495 \text{ kg (625 000 lb)}$.



(b) Minimum-shock signature. $\eta = 0.5$.

Figure 16.- Continued.



(c) Minimum-shock signature. $\eta = 0.9$.

Figure 16.- Concluded.

1. Report No. NASA TP-1820		2. Government Accession No.		3. Recipient's Catalog No.	
4. Title and Subtitle CHARTS FOR DETERMINING POTENTIAL MINIMUM SONIC-BOOM OVERPRESSURES FOR SUPERSONIC CRUISE AIRCRAFT				5. Report Date March 1981	
7. Author(s) Christine M. Darden				6. Performing Organization Code 533-01-43-04	
9. Performing Organization Name and Address NASA Langley Research Center Hampton, VA 23665				8. Performing Organization Report No. L-74190	
12. Sponsoring Agency Name and Address National Aeronautics and Space Administration Washington, DC 20546				10. Work Unit No.	
15. Supplementary Notes				11. Contract or Grant No.	
16. Abstract Charts are presented which will provide a rapid estimation of minimum achievable sonic-boom levels for supersonic cruise aircraft. These charts were obtained by using a minimization method based on modified linear theory. Results are shown for several combinations of Mach number, altitude, and aircraft length and weight. For each of these conditions, overpressure and impulse values are given for two types of sonic-boom signatures: (1) a "flat-top" or minimum-overpressure signature which has a pressure plateau behind the initial shock and (2) a minimum-shock signature which allows a pressure rise after the initial shock. Some results are also given for the effects of nose shape. An example of the use of the charts has been included.				13. Type of Report and Period Covered Technical Paper	
17. Key Words (Suggested by Author(s)) Overpressure Sonic boom				14. Sponsoring Agency Code	
18. Distribution Statement Unclassified - Unlimited				Subject Category 02	
19. Security Classif. (of this report) Unclassified		20. Security Classif. (of this page) Unclassified		21. No. of Pages 46	22. Price A03

For sale by the National Technical Information Service, Springfield, Virginia 22161

National Aeronautics and
Space Administration

THIRD-CLASS BULK RATE

Postage and Fees Paid
National Aeronautics and
Space Administration
NASA-451



Washington, D.C.
20546

Official Business

Penalty for Private Use, \$300

3 1 1U,A, 032381 S00903DS
DEPT OF THE AIR FORCE
AF WEAPONS LABORATORY
ATTN: TECHNICAL LIBRARY (SUL)
KIRTLAND AFB NM 87117

NASA

POSTMASTER: If Undeliverable (Section 158
Postal Manual) Do Not Return
